#419

IMP-H + J

HOURLY AVERAGE COUNT RATE

72-073A-06B
73-078A-06B

IMF-H

HOURLY AVERAGE COUNT RATE

72-073A-06E

THIS DATA SET HAS BEEN RESTORED. ORIGINALLY THERE WERE SEVEN 9-TRACK, 800 BPI TAPES WRITTEN IN BINARY. THERE IS ONE RESTORED TAPE. THE DR AND DS TAPES ARE 9-TRACK, 6250 BPI. THE ORIGINAL TAPES WERE CREATED ON AN IBM 370 COMPUTER. THE DR AND DS NUMBERS ALONG WITH THE CORRESPONDING D NUMBERS AND THE TIME SPANS ARE AS FOLLOWS:

DR#	DS#	D#	FILES	TIME SPAN
DR02633	DS02633	D30917	1-37	09/29/72 - 12/31/72
		D30918	38-74	01/01/73 - 12/31/73
		D30919	75-111	01/01/74 - 12/31/74
		D30922	112-148	01/01/75 - 12/31/75
		D34015	149-185	01/01/76 - 12/31/76
		D42285	186-222	01/01/77 - 12/31/77
		D47234	223-244	01/01/78 - 07/31/78

Refer to 73-078A-06B

Imp-H 047234
1/01/78 - 7/31/78

DUMP OF TAPE DO-4

INPUT TAPE DO-4 ON MT1
DATA INPUT H9 NF 22 FL 1 1 1 SR 22 1 1 SR 22 LAST 1

FILE 1 RECORD 1 LENGTH 520BYTES

(0)	00000001	00000001	FFFFFFF9	0000004E	00000001	00000001	00770525	00000000	00000000	00000000
(40)	00000000	00000000	00000000	00000000	00000000	00000000	00000000	00000000	00000000	00000000
(80)	00000000	00000000	00000000	00000000	00000000	00000000	00000000	00000000	00000000	00000000
(120)	00000000	00000000	00000000	00000000	00000000	00000000	00000000	00000000	00000000	00000000
(160)	00000000	00000000	00000000	00000000	00000000	00000000	00000000	00000000	00000000	00000000
(200)	00000000	00000000	00000000	00000000	00000000	00000000	00000000	00000000	00000000	00000000
(240)	00000000	00000000	00000000	00000000	00000000	00000000	00000000	00000000	00000000	00000000
(280)	00000000	00000000	00000000	00000000	00000000	00000000	00000000	00000000	00000000	00000000
(320)	00000000	00000000	00000000	00000000	00000000	00000000	00000000	00000000	00000000	00000000
(360)	00000000	00000000	00000000	00000000	00000000	00000000	00000000	00000000	00000000	00000000
(400)	00000000	00000000	00000000	00000000	00000000	00000000	00000000	00000000	00000000	00000000
(440)	00000000	00000000	00000000	00000000	00000000	00000000	00000000	00000000	00000000	00000000
(480)	00000000	00000000	00000000	00000000	00000000	00000000	00000000	00000000	00000000	00000000

FILE 1 RECORD 240 LENGTH 520BYTES

(0)	00000001	000000F0	00000007	0000004E	0000000A	00000018	007708C0	00000000	00000000	00000000
(40)	000009EE	000000B8	0000002F	00000009	00000031	00000005	00000001	00000000	00000001	00000000
(80)	004C59A6	00002B2E	00004249	000008E7	0005AE6A	000012DE	00000AE6	00002005	00589510	000C0235
(120)	000B17ED	000DBFF6	000F94F2	000EB264	000CC73D	000C8AEE	000C549E	000C4DDF	001D8839	02136B10
(160)	00005A86	00000441	000003E9	0000015F	00001239	00000202	00000223	000001BD	00006181	000021EF
(200)	000020D1	0000244F	000026E4	000027B7	00002301	000022AE	00002262	000022C1	000025AE	0000EED2
(240)	00000000	000003EC	00000004	00000000	00000000	00000000	00000000	433ECDE9	4147CDC6	00000000
(280)	41E21DEA	411D26CF	403B9216	3F638DA3	4046ED67	3FCACB31	3F144784	00000000	3F8F8202	00000000
(320)	4047C1D3	402262A6	3F8B0742	3F212F36	3FA21EA3	3F5AB12D	3F144784	3F145A65	3F90B989	00000000
(360)	4239E9BD	4020C159	403247EE	3F6C0F6F	4144F338	3FE50053	3F844B0D	401849F0	424330F9	4191BD83
(400)	4186A23A	41A6DF53	41BD1B09	41B25D7E	419B14BD	419838D3	4195A5A5	419553C8	42166692	43193173
(440)	4044AA07	3F33A3BB	3F2F7CE5	3F10AC8F	3FDD2D36	3F18695F	3F19F1E0	3F151B65	4049F5D5	4019BD6C
(480)	4018E462	401B8AFC	401D8043	401E202D	401A8D4E	401A4E5B	401A1528	401A5D22	401C950E	40B526EF

FILE	INPUT RECS.	DATA RECORDS INPUT	MAX. SIZE	READ ERROR SUMMARY PERM	ZERO B	SHORT	UNDEF.	INPUT RETRIES #RECS.	TOTAL#
1	240	241	520	0	0	0	0	0	0

FILE 22 RECORD 1 LENGTH 520BYTES

(0)	00000016	00000001	00000007	0000004E	000000D3	00000001	0077572D	00000000	00000000	00000000
(40)	0000003B	0000000D	00000003	00000001	00000003	00000000	00000000	00000000	0000002B	00000000
(80)	0001D89B	00001413	00001867	0000052E	000011E0	00000045	00000810	00002010	000C6548	000AA664
(120)	0002E1CA	000BD13E	000D81B9	000C8C49	000BA402	000B44FF	000ACF7F	000ABFA8	00115589	01D51140
(160)	00001003	0000034C	0000029D	00000138	0000024E	00000045	00000227	00000208	00002A1B	00002532
(200)	000013A5	000025C3	000029E4	00002D2F	000027D4	000025FA	000025C3	000024CB	00002201	00011444
(240)	00000000	00000936	000005A9	00000000	00000000	00000000	00000000	43936E66	435A9F29	00000000
(280)	4023C559	3FE09C02	3F19EA9E	3E4B64B3	3F1D9909	00000000	00000000	00000000	3F131971	00000000
(320)	3F4A82F7	3F3E4BA2	3EEF67FD	3E4B64B3	3F11169A	3F1FCA75	3EFE53B4	3E8AB947	3E3E29A3	00000000
(360)	411667B7	3FF3A719	4012829F	3F3EE868	3FD8F926	3E34A3AC	3F61DB4D	4018520B	41966FE4	41814049
(400)	4122FA0B	418F6B43	41A3EBFB	41984947	418D4642	4188C536	41833333	418272F0	41D25F48	43163CBE
(440)	3FC258ED	3F280E67	3F1FC08A	3EED3D87	3F1C02D9	3E34A3AC	3F1A273E	3F18A8F3	401FF0B7	401C3724
(480)	3FEE74F6	401CA4BF	401FC66F	4022461B	401E360D	401CCF08	401CA4BD	401BE89A	4019CB93	40D18D87

FILE 22 RECORD 48 LENGTH 520BYTES

(0)	00000016	00000030	00000007	0000004E	000000D4	00000018	007757A8	00000000	00000000	00000000
(40)	0000000A	00000003	00000000	00000000	00000000	00000000	00000001	00000000	0000002E	00000000
(80)	00010A50	00000E3C	00001423	00000402	00000347	0000006B	00000B0D	00001AF3	000BB43B	000AF3D8
(120)	0002E44C	000BDB8F	000E0A17	000CE21E	000BB109	000B5C28	000B15C4	000B10E7	0010EDCC	01DBE1F0
(160)	00000EEF	00000373	000002EF	00000144	00000128	0000006B	000002DA	00000226	00002EFD	00002C5A
(200)	0000174E	00002C4D	0000327B	0000325A	00002CE7	00002C42	00002B40	00002FC4	00002661	00013209
(240)	00000000	000006E9	000005FC	00000000	00000000	00000000	00000000	436E9666	435FC423	00000000
(280)	3F815319	3F451A0F	00000000	00000000	00000000	00000000	3EB8457F	00000000	3F135596	00000000
(320)	3F28E561	3F27E55C	3F1530F3	3EB8F105	3F18338A	3F2A61E5	3EB8457F	3EB8F105	3E390580	00000000

```
(   360)   40CA0145  3FACC8BC  3FF46672  3F30A565  3F27D247  3E514F67  3F862602  4014718B  418E0B2D  4184EC4E
(   400)   4123187C  418FE875  41AA62F5  419C5AF8  418DE468  4189DE46  41868800  41864CFB  41CD7445  43168F74
(   440)   3FB53EF7  3F29E803  3F23A640  3EF621BF  3EE1438E  3E514F67  3F22A311  3F1A1AEB  4023A445  4021A4DD
(   480)   4011AD82  40219A8C  40264A70  402631DD  40220F46  402192C0  4020CE66  40243BD0  401D1C83  40E82296

        FILE   INPUT    DATA RECORDS    MAX.          READ ERROR SUMMARY          INPUT RETRIES
               RECS.      INPUT        SIZE       PERM  ZERO B   SHORT  UNDEF.  #RECS.  TOTAL#
          22      48       49           520         0       0       0       0       0       0

 EOJ        DUMP STOPPED AFTER FILE   22        # OF PERMANENT READ ERRORS  0

START TIME 02/19/82  15:59:32        STOP TIME 02/19/82  16:00:58

$$
$ASS BI MT4 BO TPL
$EXE XFER.N BS
```

IMP-J

HOURLY AVERAGE COUNT RATES

73-078A-06B

THIS DATA SET HAS BEEN RESTORED. THERE WERE ORIGINALLY 19 9-TRACK, 1600 BPI TAPES, WRITTEN IN BINARY. THERE ARE FOUR RESTORED TAPES. THE DR TAPES ARE 3480 CARTRIDGES AND THE DS TAPES ARE 9-TRACK, 6250 BPI. THE ORIGINAL TAPES WERE CREATED ON AN IBM 360 COMPUTER. THE DR AND DS NUMBERS ALONG WITH THE CORRESPONDING D NUMBERS AND TIME SPANS ARE AS FOLLOWS:

DR#	DS#	DD#	FILES	TIME SPAN
DR004185	DS004185	D030920	1-37	10/28/73 - 12/31/73
		D030923	38-74	01/01/74 - 12/31/74
		D030924	75-111	01/01/75 - 12/31/75
		D034016	112-148	01/01/76 - 12/31/76
		D042286	149-185	01/01/77 - 12/31/77
DR004186	DS004186	D047235	1-37	01/01/78 - 12/31/78
		D054735	38-74	01/01/79 - 12/31/79
		D057300	75-111	01/01/80 - 12/31/80
		D080589	112-148	01/01/81 - 12/31/81
		D086638	149-185	01/01/82 - 12/31/82
DR004187	DS004187	D086639	1-2	01/01/83 - 12/31/83
		D080619	3-39	01/01/84 - 12/31/84
		D080590	40-76	01/01/85 - 12/31/85
		D080591	77-113	01/01/86 - 12/31/86
		D080620	114-150	01/01/87 - 12/31/87
DR004188	DS004188	D080592	1-37	01/01/88 - 12/31/88
		D080110	38-74	01/01/86 - 12/31/86
		D083159	75-111	01/01/89 - 12/31/89
		D083158	112-148	01/01/90 - 12/31/90

California Institute of Technology
Space Radiation Laboratory
Pasadena, CA 91125
9/2/93

To: Ralph Post
From: Dick Mewaldt R.A. Mewaldt
Subject: Replacement Tape for 1990 data from the Caltech Experiment on IMP-8

Enclosed is a replacement tape containing data for the year 1990 from our experiment on IMP-8. I hope you are able to read it and apologize for the delay in processing it.

DD-83158
73-078A-06B

IMP-J

HOURLY AVERAGE COUNT RATE

73-078A-06B

THIS DATA SET CATALOG CONSISTS OF 17 IMP-J TAPES. THE TAPES, PREVIOUS TO 1981 DATA, ARE 9-TRACK, 800 BPI, BINARY FORMAT WITH 37 FILES(UNLESS OTHERWISE NOTED), AND CREATED ON AN IBM/360 COMPUTER. HOWEVER, DATA FPR, 1981 AND FORWARD WERE WRITTEN ON A VAX COMPUTER AT 1600 BPI.

D#	C#	TIMESPANS
D-30920	C-19731	10/28/73-12/31/73
D-30923	C-19732	01/01/74-12/31/74
D-30924	C-19733	01/01/75-12/31/75
D-34016	C-20643	01/01/76-12/31/76
D-42286	C-21307	01/01/77-12/31/77
D-47235	C-22143	01/01/78-12/31/78
D-54735	C-22953	01/01/79-12/31/79
D-57300	C-23125	01/01/80-12/31/80
*** TAPES FORM THIS POINT ON, ARE 1600 BPI, VAX CREATED ***		
D-80589	C-27796	01/01/81-12/31/81
D-86638	C-030220	01/01/82-12/31/82
D-86639	C-030221	01/01/83-12/31/83
D-80619	C-28056	01/01/84-12/31/84
D-80590	C-27797	01/01/85-12/31/85
D-80591	C-27798	01/01/86-12/31/86
D-80620	C-28057	01/01/87-12/31/87
D-80592	C-27799	01/01/88-12/31/88
D-83159	C-28058	01/01/89-12/31/89

*** D-80110 C-27534 TO BE REUSED WHEN NEW DATA COMES IN ***
ALSO D-83158 IS PENDING 1990 full year of data

CALIFORNIA INSTITUTE OF TECHNOLOGY

GEORGE W. DOWNS LABORATORY OF PHYSICS

July 28, 1989

Ralph Post
National Space Science Data Center
Goddard Space Flight Center
Code 601
Greenbelt, Maryland 20771

Dear Ralph,

Under separate cover we have shipped to you one magnetic tape labeled "IMP-8 EIS 1986" which we are submitting to the NSSDC from our Caltech Experiment on IMP-8. It includes hourly-averaged fluxes and counting rates for the period from 1986:001 to 1986:365. Please note that while this tape contains the same quantities that were included in our earlier submissions for the years 1972 to 1980, it is written in a new format. This new format is described in the attached material, which should be considered an addendum to the document entitled "Data Submission to the NSSDC from the Caltech Electron/Isotope Spectrometer on IMP-7 and IMP-8" (originally submitted in 12/77).

This 1986 data is intended in part as a test of new software and of this new format (we had originally intended to furnish 1981 data for this test but 1986 turned out to be more convenient). If we do not hear from you in the next two months we will assume that this tape is readable and we will continue submitting data from the rest of the years 1981 to 1988 on a regular schedule.

Please call me at 818-356-6612 if you have any questions.

With best regards,

R. A. Mewaldt

Richard Mewaldt

xc: J. King, E. C. Stone

PASADENA, CALIFORNIA 91125

V. DESCRIPTION OF DATA ON MAGNETIC TAPE

A1. Tape Format (Revised for 1981 and after)

Data for 1981 and the following years were written in a revised format, described in Table 9. As before, one record is written for each hour; records are grouped into files of 10 days in length to facilitate searching for a particular date. One tape is provided for each calendar year and for each of the two satellites. Note that records are written for hours in which no data was available; these records are flagged by negative identification fields (IDSAT). Files which contain no data have only one record.

The new tapes for 1981 and thereafter are 9-track, 1600 bytes per inch. They are generated by a program run on a microvax. The quantities marked data type I in the table are 4-byte, 32-bit integers. Those marked data type R are 4-byte floating point.

TABLE 9

IMP EIS DATA
TAPE RECORD FORMAT
(starting 1981)

Item No.	Data Type	Mnemonic	Description and Comments
1	I	IFN	File number, from 1 to 37, 10 days per file
2	I	IRN	Record number, from 1 to 240, 1 hour per record
3	I	IDSAT	Satellite identification 7 or -7 -> IMP-7 = IMP-H 8 or -8 -> IMP-8 = IMP-J
4	I	IYEAR	Year, from 72 up
5	I	IDY	Day, from 1 to 366
6	I	IHR	Hour, from 1 to 24
7	I	ITIME	Time, from 7200101 up, = 100000*IYEAR+100*IDY+IHR
8-10	-		Spare
			Event counts:
11	I	KNT(1)	D2 protons, 1.43-2.34 MeV
12	I	KNT(2)	D25 protons, 2.5-4.0 Mev
13	I	KNT(3)	D25 protons, 4.0-7.0 MeV
14	I	KNT(4)	D25 protons, 7.0-12.5 MeV
15	I	KNT(5)	D2 alphas, 1.43-2.34 MeV/nuc
16	I	KNT(6)	D25 alphas, 2.5-4.0 MeV/nuc
17	I	KNT(7)	D25 alphas, 4.0-7.0 MeV/nuc
18	I	KNT(8)	D25 alphas, 7.0-12.5 MeV/nuc
19	I	KNT(9)	D01* electrons, ~1-5 MeV
20	-		Spare
21	-		Spare
22	I	LTNG	Narrow geometry live time in sec
23	I	LTWG	Wide geometry live time in sec
24-7	-		Spare
28	R	TLNG	Narrow geomtetry live time in sec
29	R	TLWG	Wide geometry live time in sec
30	-		Spare
			Fluxes:
31	R	FLX(1)	D2 protons, 1.43-2.34 MeV
32	R	FLX(2)	D25 protons, 2.5-4.0 Mev
33	R	FLX(3)	D25 protons, 4.0-7.0 MeV
34	R	FLX(4)	D25 protons, 7.0-12.5 MeV
35	R	FLX(5)	D2 alphas, 1.43-2.34 MeV/nuc
36	R	FLX(6)	D25 alphas, 2.5-4.0 MeV/nuc
37	R	FLX(7)	D25 alphas, 4.0-7.0 MeV/nuc
38	R	FLX(8)	D25 alphas, 7.0-12.5 MeV/nuc
39	R	FLX(9)	D01* electrons, ~1-5 MeV
40	-		Spare

Item No.	Data Type	Mnemonic	Description and Comments
			Uncertainty in fluxes:
41	R	UFLX(1)	D2 protons, 1.43-2.34 MeV
42	R	UFLX(2)	D25 protons, 2.5-4.0 Mev
43	R	UFLX(3)	D25 protons, 4.0-7.0 MeV
44	R	UFLX(4)	D25 protons, 7.0-12.5 MeV
45	R	UFLX(5)	D2 alphas, 1.43-2.34 MeV/nuc
46	R	UFLX(6)	D25 alphas, 2.5-4.0 MeV/nuc
47	R	UFLX(7)	D25 alphas, 4.0-7.0 MeV/nuc
48	R	UFLX(8)	D25 alphas, 7.0-12.5 MeV/nuc
49	R	UFLX(9)	D01* electrons, ~1-5 MeV
50	-		Spare
			Rates, counts per sec:
51	R	R(1)	D0*
52	R	R(2)	D01*
53	R	R(3)	ELO
54	R	R(4)	EHI
55	R	R(5)	PLO
56	R	R(6)	PHI
57	R	R(7)	PEN
58	R	R(8)	NEUT
59	R	R(9)	D0
60	R	R(10)	D1
61	R	R(11)	D2
62	R	R(12)	D3
63	R	R(13)	D4
64	R	R(14)	D5
65	R	R(15)	D6
66	R	R(16)	D7
67	R	R(17)	D8
68	R	R(18)	D9
69	R	R(19)	D10
70	R	R(20)	D11
			Uncertainty, counts per sec:
71	R	RU(1)	D0*
72	R	RU(2)	D01*
73	R	RU(3)	ELO
74	R	RU(4)	EHI
75	R	RU(5)	PLO
76	R	RU(6)	PHI
77	R	RU(7)	PEN
78	R	RU(8)	NEUT
79	R	RU(9)	D0
80	R	RU(10)	D1
81	R	RU(11)	D2
82	R	RU(12)	D3
83	R	RU(13)	D4
84	R	RU(14)	D5
85	R	RU(15)	D6
86	R	RU(16)	D7
87	R	RU(17)	D8
88	R	RU(18)	D9
89	R	RU(19)	D10
90	R	RU(20)	D11

SRL TECHNICAL REPORT 77-2

DATA SUBMISSION TO THE NSSDC FROM THE CALTECH ELECTRON/ISOTOPE SPECTROMETER ON IMP-7 AND IMP-8

T. L. Garrard
R. A. Mewaldt
E. C. Stone
R. E. Vogt

California Institute of Technology
Pasadena, California 91125

December 4, 1977

DATA SUBMISSION TO THE NSSDC
FROM THE CALTECH ELECTRON/ISOTOPE SPECTROMETER
ON IMP-7 AND IMP-8

OUTLINE

I. Introduction

II. Description of the Experiments

- A. The Detector Telescope
- B. Orientation on the Spacecraft
- C. Discriminators and Analyzers
- D. IMP-8 EIS: Special Features

III. Description of Counting Rates

IV. Description of Rate Plots

- A. Singles Rates
- B. Orbit and Coincidence Rates
- C. Interpretation of ELO and EHI Electron Rates
- D. Electron Response of the DO* and DO1* Rates

V. Description of Data on Magnetic Tape

- A. Tape Format
- B. Interpretation of Hourly Average Count Rates and Fluxes
- C. Corrections to the Flux of 1.43 - 2.34 MeV/nuc Protons and Alphas
- D. Interpretations of 1-5 MeV Electron Fluxes

VI. Bibliography

Tables

Figures

I. INTRODUCTION

Caltech is furnishing data from the Electron/Isotope Spectrometers (EIS) on IMP's 7 and 8 to the NSSDC in the form of microfilmed rate plots and selected count rates on magnetic tape. This report describes the Caltech experiments briefly. The rate plots and the tapes are described in some detail. A bibliography is provided for the user who wishes additional information.

The Principle Investigator for the EIS instruments is E. C. Stone, with R. E. Vogt as Co-investigator. Analog Technology Corporation was responsible for the detailed design and fabrication of the instrument. This work was supported in part by NASA under contract NAS5-11066 and Grant 05-002-160.

II. DESCRIPTION OF THE EXPERIMENTS

This report describes the Caltech experiments on IMP-7 (IMP-H) and IMP-8 (IMP-J). The two experiments are quite similar. The IMP-7 experiment will be described first and then the differences between 7 and 8 will be described.

A. The Detector Telescope

The Caltech IMP-7 EIS consists of eleven solid-state detectors in a stack, surrounded by a plastic scintillator anticoincidence counter (D11) in a "telescope" arrangement as illustrated in Figure 1a. Detectors D0, D1, D3, and D4 are annular devices. Nominal detector properties are given in Table 1.

All of the solid-state detectors are silicon surface-barrier detectors with negligible dead layers. An aluminized mylar window (~2.4 mg/cm^2 thick) protects the detectors from sunlight and excludes very low-energy particles.

The EIS has three modes of operation--labeled Narrow Geometry, Wide Geometry, and Neutral. These are defined in Table 2 in terms of detector requirements.

Narrow Geometry events are due to particles which entered the telescope through the aperture of the annulars and are analyzed in detectors D2 and D5 through D9. This mode has the best defined geometry (but the smallest geometrical factor). Unambiguous separation of electrons and nuclei is possible in this mode because the 50-micron detector, D2 , is sensitive to low-energy nuclei, but not to electrons.

Wide Geometry events must trigger D0 and then stop before triggering D10 or D11. These events have a much larger geometrical factor.

Events analyzed in the Neutral analysis mode must trigger D7 without triggering D5, D10, or D11. This mode is used to monitor the background due to neutral particles such as gamma rays and neutrons which interact in the detector stack after being generated by the nuclear interaction of high-energy cosmic rays in the spacecraft.

B. Orientation on the Spacecraft

The telescope acceptance direction (telescope axis) is oriented perpendicular to the spacecraft spin axis, which is approximately normal to the ecliptic, so that the instrument scans the cosmic-ray fluxes in all directions in the ecliptic as the spacecraft spins. The ecliptic plane is divided into 8 equal sectors and each event is tagged according to its sector of incidence.

C. Discriminators and Analyzers

All pulse height analyzers (PHA's) except D2 and D5 have 1024 channel ADC's with channel widths of about 160 KeV. The D2 and D5 PHA's have 4096 channels with a channel width of about 40 KeV. Except D2 and D5, all discriminators have thresholds set well below the level corresponding to normally incident minimum ionizing particles, but above the noise. D2 and D5 have high and low thresholds to allow discrimination between minimum ionizing particles and low-energy nuclei. Table 3 specifies nominal thresholds for the discriminators.

D. IMP-8 EIS : Special Features

The most notable difference between the IMP-7 and IMP-8 instruments is the rearrangement of detectors (see Figure 1b). This rearrangement provides for a significantly increased geometrical factor in the narrow geometry mode. Note that the IMP-7 and 8 EIS logic is identical; therefore, the detector labels in Figures 1a and 1b have the same logical significance.

Table 4 lists nominal detector properties for the IMP-8 EIS.

The D2H threshold is 300 KeV on the IMP-8 EIS. As noted above, logical requirements for modes of operation have not changed. The interpretation of these modes is modified as detailed in Table 5.

The IMP-8 aluminized-Mylar window is ~ 3.2 mg/cm^2 thick.

III. DESCRIPTION OF COUNTING RATES

Counting rates are accumulated for all single detector triggers and for the coincidence rates listed in Tables 6 and 7. In addition, HAZ, the rate of events with hazard flags, and ADC, the rate for triggering any solid state detector, are accumulated.

The ELO, EHI, PLO, PHI, DO*, DO1*, PEN, D5, D2H, ADC, and D11 rates are sectored.

Tables 6 and 7 describe the nominal response to incident particles. Background is fairly well known for the IMP-7 rates, less study (at this time) has been made of the IMP-8 background.

The busy signal mentioned in the tables indicates event analysis is in progress. The dead time due to this analysis is typically ~10 milliseconds out of 640 milliseconds.

8

IV. DESCRIPTION OF RATE PLOTS

Two pages of plots are supplied for each time period covered, including single detector rates and orbit parameters and coincidence rates. Plots are furnished with two different time scales - about 4 to 8 days per page or about 28 days per page (called solar rotation plots). Examples of the plots are shown in the figures and discussed below.

A. Singles Rates

This plot shows the counting rate of all discriminators and the ADC and HAZ rates (described in Section III). Rates are plotted in counts per second vs time in days.

B. Orbit and Coincidence Rates

These plots have the coincidence rates described in Section III and some orbital position parameters. The sun-earth-satellite angle in degrees is shown on all plots. Many of these plots also show the GSM θ and ϕ coordinates of the satellite. These coordinates are time-averaged before plotting, which accounts for the histogram-like appearance and the obvious problem at the point where ϕ goes from 360° to 0°.

The PLO and PHI rates may, with reasonable accuracy, be converted to proton intensities using the energy intervals and geometrical factors specified in Tables 6 and 7. A minor inaccuracy in this procedure is the inclusion of alpha particles and other heavy nuclei.

The EIS electron rates cannot be treated in such a straightforward fashion because of electron scattering. Algorithms for derivation of electron intensity spectra from ELO and EHI and DO* and DO1* are provided in sections IV.C and IV.D.

C. Interpretation of the ELO and EHI Electron Rates

Because of the large amount of scattering undergone by low energy electrons, the ELO and EHI responses are somewhat energy dependent. Therefore, the threshold and geometrical factor information given in Tables 6 and 7 represents only typical values. A more quantitative interpretation of the electron rates is possible using Figures 4 and 5, which incorporate detailed prelaunch calibration data obtained with monoenergetic electron beams.

Figure 4 shows the IMP-7 ELO and EHI rates, and the EHI/ELO ratio as a function of the spectral index γ for electron spectra of the form $\frac{dJ}{dE} = 1.0\ E^{-\gamma}$, where $\frac{dJ}{dE}$ is the differential flux $(cm^2\text{-sec-sr-MeV})^{-1}$ and E is the kinetic energy in MeV.

The procedure for using Figure 4 is as follows:

1) Subtract off the ELO and EHI neutral background contributions using the NEUT rate and

$$\text{ELO (Bkgd)} = (0.55 \pm 0.01)\ \text{NEUT}$$

$$\text{EHI (Bkgd)} = (0.20 \pm 0.01)\ \text{NEUT}$$

(When D7 is off, use NEUT $\simeq$ 0.010 x D8 singles rate.)

2) Determine the spectral index γ from the EHI/ELO ratio (background corrected) and the left hand vertical scale.

3) For this value of γ, use either the ELO or EHI rates (right hand vertical scale) to obtain the absolute intensity normalization.

Example: Figure 3a, Day 102, Time 13:00-13:30

Rate Name	Figure 3a (Counts/sec)	Background Contribution	Electron Contribution (Counts/sec)
ELO	1.9	.06	1.84
EHI	0.11	.02	0.09
NEUT	0.10		
ELO/EHI = 0.049			=> $\gamma \approx 3.2$

Thus, a spectrum of the form $dJ/dE \simeq 3\ E^{-3.2}\ (cm^2\text{-sec-sr-MeV})^{-1}$ is consistent with the electron rates observed during this period.

Note: Because of the large neutral background contribution to ELO and EHI, this procedure is justified only when these rates are significantly above background level.

Figure 5 shows the corresponding ELO and EHI response curves for the IMP-8 EIS. Calibrations of the IMP-8 EIS electron response were performed from 0.1 to ~ 10 MeV. Background corrected electron rates can be obtained from the following:

$$\text{ELO (Bkgd)} = (0.60 \pm 0.02)\ \text{NEUT}$$

$$\text{EHI (Bkgd)} = (0.21 \pm 0.01)\ \text{NEUT}$$

11

D. Electron Response of the DO* and DO1* Rates

Figures 6 (IMP-7) and 7 (IMP-8) show the response of the DO* and DO1* rates to electron spectra of the form $dJ/dE = 1.0\ E^{-\gamma}\ (cm^2\text{-sec-sr-MeV})^{-1}$. Because of their larger geometry factors, these wide geometry rates are sometimes more useful than the ELO and EHI rates for obtaining approximate electron spectra. The neutral background corrections to DO* and DO1* are shown below.

A difficulty in using the wide geometry rates is that they also respond to nuclei (see Tables 6 and 7), which often dominate the interplanetary particle fluxes. First order estimates of the contributions of cosmic ray nuclei to DO* can be derived from the PLO and PHI rates, as shown below. The 13-43 MeV/nuc corrections for DO1* are typical quiet time values, and would not apply during large solar flares. Reliable electron fluxes can be derived from the DO* and DO1* rates only if the estimated contribution of nuclei is small ($\leqslant$ 20%) compared to the total counting rates. If the nuclei contribution is comparable to that of electrons, pulse height information (not included in the rate plots) is required to isolate the electron and nuclei contributions.

Wide Geometry Electron Background Corrections

Background Contributions	Wide Geometry Rate	Count Rate (sec^{-1}) IMP-7	IMP-8
Neutral Particles	DO*	(1.0 ± .1) NEUT	(1.0 ± .1) NEUT
	DO1*	(0.20 ± .01) NEUT	(0.235 ± .010) NEUT
H + He Nuclei (1-13 MeV/nuc)	DO*	~ 10 x PLO + 30 x PHI	~ 6 (PLO + PHI)
H + He Nuclei (13-43 MeV/nuc)	DO*, DO1*	~ 0.003	~ 0.003

V. DESCRIPTION OF DATA ON MAGNETIC TAPE

A. Tape Format

Magnetic tapes containing rates and/or fluxes of various types of events are furnished in addition to the rate plots. Table 8 describes the tape format. One record is written for each hour; records are grouped into files of 10 days in length to facilitate searching for a particular date. One tape is provided for each calendar year and for each of the two satellites. Note that records are written for hours in which no data was available; these records are flagged by negative identification fields, item 3 in Table 8. Files which contain no data have only one record.

The tapes are 9-track, 800 bytes per inch. They are generated by an IBM 370/158 program using a RECFM=F, BLKSIZE=520 specification. The quantities marked data type I are 4-byte, 32-bit binary integers. The quantities marked data type R are 4-byte IBM 370 floating-point, REAL*4 variables. Sufficient data is given in the I format to allow users without access to an IBM 360 or 370 to re-calculate all floating-point quantities without the necessity of a floating-point format conversion.

The rates given (items 21-40 and 91-110) are described in sections III and IV. The event counts (items 11-19) and the fluxes derived from them (71-99) are based on event data with pulse-height analysis. These fluxes are described in Section V.B, following.

B. DESCRIPTION OF HOURLY AVERAGE COUNT RATES AND FLUXES

The magnetic tapes submitted from the two EIS instruments contain hourly event totals, count rates and absolute fluxes for the following particle types:

Particle	Energy Range
Protons	1.43-2.34 MeV
	2.5 - 4.0 "
	4.0 - 7.0 "
	7.0 -12.5 "
Alphas	1.43-2.34 MeV/nuc
	2.5 - 4.0 "
	4.0 - 7.0 "
	7.0 -12.5 "
Electrons	~ 1 - 5 MeV

These event totals are based on the analysis of pulse-height and range information for individual events recorded by the EIS instruments. The coincidence counting rates described in Section III and IV and Tables 6 and 7 have been used to normalize the absolute fluxes.

In addition, hourly average count rates of all EIS single detector and coincidence rates are provided.

C. CORRECTIONS TO THE FLUX OF 1.43-2.34 MeV/nuc PROTONS AND ALPHAS

The count rates and fluxes submitted for 1.43-2.34 MeV/nuc protons and alpha particles are based on pulse-height analysis of the 50μm detector D2, and thus represent an inherently single parameter measurement. If absolute fluxes in this energy interval are required, the following corrections should be considered.

C.1. Alpha Particle Contamination of D2 Proton Fluxes

In the IMP-8 EIS, for example, the flux of 1.43-2.34 MeV protons is based on the count rate of particles which deposit 0.50 to 1.85 MeV in D2. This D2 pulse height interval also responds to incident alpha particles with 1.27 to 1.40 MeV/nuc. The alpha particle contribution to the proton counting rate depends on the alpha particle intensity and spectrum, but is normally small. Table 9 summarizes the relevant pulse height and energy intervals for the IMP-7 and 8 instruments. Figure 8 shows the ratio

$$\frac{(\alpha \text{ contribution to } 1.43 - 2.34 \text{ MeV proton flux})}{(1.43 - 2.34 \text{ MeV/nuc } \alpha \text{ flux})}$$

as a function of spectral index γ, assuming spectra of the form $\frac{dJ}{dE} \propto E^{-\gamma}$.

More explicitly, Figure 8 shows

$$\text{FLUX RATIO} = \frac{\int_{1.27}^{1.40} E^{-\gamma} dE}{\int_{1.43}^{2.34} E^{-\gamma} dE} \quad \text{for IMP-8}$$

and

$$\text{FLUX RATIO} = \frac{\int_{1.11}^{1.25} E^{-\gamma} dE}{\int_{1.43}^{2.34} E^{-\gamma} dE} \quad \text{for IMP-7}$$

Note that since the magnitude of this contamination is of the order of the alpha to proton ratio, corrections for this effect are probably not warranted except during alpha-rich periods ($\alpha/p \gtrsim 0.1$).

Energy Intervals for Proton Fluxes Derived from D2

S/C	D2 Pulse Height (MeV)	Proton Energy Interval (MeV)	Alpha Energy Interval (MeV/nuc)
7	0.58 - 1.97	1.44 - 2.33	1.11 - 1.25
8	0.50 - 1.85	1.43 - 2.34	1.27 - 1.40

C.2. "Foldback" Correction for IMP-7

A second correction which applies only to IMP-7, is due to particles which pass through D2 and stop in inactive material without triggering D3,D4, or D5. In other words, a fraction of higher energy (> 2.4 MeV/nuc) protons and alphas will deposit an energy in D2 corresponding to lower energy (< 2.4 MeV/nuc) stopping nuclei. The energy interval within which this "foldback" effect contributes to the 1.43-2.34 MeV/nuc count rates is 2.4 - 4.5 MeV/nuc. The magnitude and energy dependence of this effect was measured during accelerator calibrations of the IMP-7 EIS and has been verified using flight data. To correct for this contamination, subtract 1.1 ± 0.1 times the 2.5 - 4.0 MeV/nuc proton (alpha) flux (units of $cm^{-2}sr^{-1}sec^{-1}$ MeV/nuc^{-1}) from the corresponding flux in the 1.43-2.34 MeV/nuc proton (alpha) interval. Note that the relative size of the correction is greatest for hard spectra. For $dJ/dE \propto E^{-3}$, the correction amounts to ~ 18% of the total count rate. This correction does not apply to IMP-8.

C.3. IMP-7 D2 Offset Shift

During the period 73:096 to 73:155 an offset shift in the IMP-7 D2 ADC was observed. The effect of this shift, which had also been observed during prelaunch calibrations, was to shift the energy threshold of all D2 channels down by a constant amount corresponding to ~ 3 channel widths. Therefore the effective energy interval for D2 protons during this period is 1.36 to 2.22 MeV instead of the nominal 1.43 - 2.34 MeV. A similar shift occurred during the period 75:101 to 75:172. Data for all other periods have the nominal energy calibration.

For spectra of the form $dJ/dE \propto E^{-\gamma}$, the reported flux during the period of the shift will be higher than that for the nominal energy interval by a factor ranging from 1.01 (γ=1) to 1.24 (γ=5). If desired, a correction factor of x0.88 (corresponding to a typical value of γ=3) can be applied. A second consequence of this offset shift is that the reported fluxes of 7-12.5 MeV protons during these periods is not reliable.

17

D. INTERPRETATION OF 1-5 MeV ELECTRON FLUXES

The 1-5 MeV electron fluxes submitted on tape are derived from the wide geometry analysis mode and include events that trigger D0 and then stop in D1 through D9. Pulse height data have been used to separate electron-like events from nuclei. The 1-5 MeV electron fluxes and events totals have been corrected for neutral particle background as described in Section IV.D. Since August, 1975, hourly average fluxes of 1-5 MeV electrons have been submitted to the Solar-Geophysical Data Bulletin each month.

Note that this energy interval frequently responds to magnetospheric electrons, as seen, for example, in Figures 2b and 3b. Such periods can usually be identified by inspection of count rates such as EL0 and D0*, which respond to ≥ 0.2 MeV electrons, or by comparing IMP-7 and IMP-8.

During periods when the counting rates are high, the wide geometry live time may be small or zero due to the lower priority of wide geometry events. In such cases the background corrected 1-5 MeV electron rate may be zero or negative due to statistical fluctuations. The reported fluxes for these hours have been set equal to zero with an uncertainty corresponding to a 1σ upper limit. During some of these periods usable 1-5 MeV electron fluxes may be obtained from the EHI rate (Section IV.C.).

IMP 7 & 8 BIBLIOGRAPHY

CALTECH ELECTRON/ISOTOPE SPECTROMETER

November 1977

"Observations of 0.16 to 3 MeV Electrons during Solar Quiet Times", G. J. Hurford, R. A. Mewaldt, E. C. Stone, and R. E. Vogt, Bull. Am. Phys. Soc., 18, 568 (1973).

"Observations of the Ratio of Low-Energy Cosmic Ray Positrons and Electrons", G. J. Hurford, R. A. Mewaldt, E. C. Stone, and R. E. Vogt, Bull. Am. Phys. Soc., 18, 569 (1973).

"The Energy Spectrum of 0.16 to 3 MeV Electrons during Solar Quiet Times", G. J. Hurford, R. A. Mewaldt, E. C. Stone, and R. E. Vogt, Conf. Papers, 13th Int'l Cosmic Ray Conference, Denver, 1, 324 (1973).

"Observations of the Ratio of Low-Energy Cosmic Ray Positrons and Electrons during Solar Quiet Times", G. J. Hurford, R. A. Mewaldt, E. C. Stone, and R. E. Vogt, Conf. Papers, 13th Int'l Cosmic Ray Conference, Denver, 1, 330 (1973).

"Observations of the Time-Variations and Anisotropy of 0.16 to 3 MeV Electrons", G. J. Hurford, R. A. Mewaldt, E. C. Stone, and R. E. Vogt, Conf. Papers, 13th Int'l Cosmic Ray Conference, Denver, 1, 334 (1973).

"Observations of Low Energy Hydrogen and Helium Isotopes during Solar Quiet Times", G. J. Hurford, R. A. Mewaldt, E. C. Stone, and R. E. Vogt, Conf. Papers, 13th Int'l Cosmic Ray Conference, Denver, 1, 93 (1973).

"Measurements of the Flux of Low-Energy Solar-Flare Positrons", G. J. Hurford, R. A. Mewaldt, E. C. Stone, and R. E. Vogt, Conf. Papers, 13th Int'l Cosmic Ray Conference, Denver, 2, 1613 (1973).

"Observations of H and He Isotopes in Solar Cosmic Rays", G. J. Hurford, R. A. Mewaldt, E. C. Stone, and R. E. Vogt, Bull. Am. Astron. Soc., Part II, 6, 270 (1974).

"Observations of Low-Energy Hydrogen and Helium Nuclei during Solar Quiet Times", G. J. Hurford, R. A. Mewaldt, E. C. Stone, and R. E. Vogt, Bull. Am. Astron. Soc., Part II, 6, 274 (1974).

"The Time Variation of 5-11 MeV/nucleon Cosmic Ray Nitrogen and Oxygen Nuclei", R. A. Mewaldt, E. C. Stone, and R. E. Vogt, Bull. Am. Phys. Soc., 19, 433 (1974).

"The Isotopic Composition of 5 to 12 MeV/nucleon Cosmic Ray Nitrogen and Oxygen Nuclei", G. J. Hurford, R. A. Mewaldt, E. C. Stone, S. B. Vidor, and R. E. Vogt, Bull. Am. Phys. Soc., 19, 433 (1974).

"The Energy Spectrum of 0.16 to 2 MeV Electrons during Solar Quiet Times", G. J. Hurford, R. A. Mewaldt, E. C. Stone, and R. E. Vogt, Ap. J., 192, 541 (1974).

"Observations of Low Energy Hydrogen and Helium Isotopes during Solar Quiet Times", G. J. Hurford, R. A. Mewaldt, E. C. Stone, and R. E. Vogt, presented at the 2nd Cosmic Ray Isotope Symposium, Durham, N. H., October 1974.

"Isotopic Composition of 6-12 MeV/nuc Cosmic Ray Nitrogen and Oxygen", R. A. Mewaldt, E. C. Stone, S. B. Vidor, and R. E. Vogt, presented at the 2nd Cosmic Ray Isotope Symposium, Durham, N. H., October 1974.

"Isotopic Calibration of a dE/dx-E Telescope", R. A. Mewaldt, E. C. Stone, S. B. Vidor, and R. E. Vogt, presented at the 2nd Cosmic Ray Isotope Symposium, Durham, N. H., October 1974.

"Solar Cosmic Ray Observations of Hydrogen and Helium Isotopes", G. J. Hurford, E. C. Stone, and R. E. Vogt, presented at the 2nd Cosmic Ray Isotope Symposium, Durham, N. H., 1974.

"The Anomalous Low-Energy Cosmic Rays: Local or Interstellar?", R. A. Mewaldt, Invited Paper, Anaheim APS Meeting, Bull. Am. Phys. Soc., 20, 52 (1975).

"Observations of Hydrogen and Helium Isotopes in Low-Energy Cosmic Rays", R. A. Mewaldt, E. C. Stone, and R. E. Vogt, Bull. Am. Phys. Soc., 20, 709, (1975).

"The Elemental Composition of Cosmic Rays with 3-30 MeV/nuc", E. C. Stone, R. A. Mewaldt, S. B. Vidor, and R. E. Vogt, ibid, 20, 633 (1975).

"The Puzzle of ^{3}He Rich Solar Flares", E. C. Stone, Invited Paper, Washington APS Meeting, April 1975, Bull. Am. Phys. Soc., 20, 680 (1975).

"A Search for Solar Flare Positrons", R. A. Mewaldt, E. C. Stone, and R. E. Vogt, 14th Int'l Cosmic Ray Conference, Munich, Germany, Conf. Papers, Vol. 5, p. 1668, (1975).

"Implications of Time Variations for the Origin of Low Energy Cosmic Ray Nitrogen and Oxygen Nuclei", R. A. Mewaldt, E. C. Stone, and R. E. Vogt, 14th Int'l Cosmic Ray Conference, Munich, Germany, Conf. Papers, Vol. 2, p. 798, (1975).

"The Quiet Time Spectra of Low-Energy Hydrogen and Helium Nuclei", R. A. Mewaldt, E. C. Stone, and R. E. Vogt, 14th Int'l Cosmic Ray Conference, Munich, Germany, Conf. Papers, Vol. 2, p. 774, (1975).

"The Isotopic Composition of Hydrogen and Helium in Low-Energy Cosmic Rays", R. A. Mewaldt, E. C. Stone, and R. E. Vogt, 14th Int'l Cosmic Ray Conference, Munich, Germany, Conf. Papers, Vol. 1, p. 306, (1975).

"Observations of Low Energy Interplanetary Electrons", R. A. Mewaldt, E. C. Stone, and R. E. Vogt, 14th Int'l Cosmic Ray Conference, Munich, Germany, Conf. Papers, Vol. 2, p. 758, (1975).

"The Elemental Composition of 4 - 30 MeV/nuc Cosmic Ray Nuclei with $1 \leq Z \leq 8$", R. A. Mewaldt, E. C. Stone, S. B. Vidor, and R. E. Vogt, 14th Int'l Cosmic Ray Conference, Munich, Germany, Conf. Papers, Vol. 2, p. 798 (1975).

"Isotopic Composition of the Anomalous Low-Energy Cosmic Ray Nitrogen and Oxygen", R. A. Mewaldt, E. C. Stone, S. B. Vidor, and R. E. Vogt, 14th Int'l Cosmic Ray Conference, Munich, Germany, Conf. Papers, Vol. 1, p. 349 (1975).

"Observations of Hydrogen and Helium Isotopes in Solar Cosmic Rays", G. J. Hurford, E. C. Stone, and R. E. Vogt, 14th Int'l Cosmic Ray Conference, Munich, Germany, Conf. Papers, Vol. 5, p. 1624 (1975).

"The Quiet Time Flux of 0.16 - 1.6 MeV Cosmic Ray Positrons", R. A. Mewaldt, E. C. Stone, and R. E. Vogt, 14th Int'l Cosmic Ray Conference, Munich, Germany, Conf. Papers, Vol. 1, p. 401 (1975).

"Enrichment of Heavy Nuclei in ^{3}He Rich Flares", G. J. Hurford, R. A. Mewaldt, E. C. Stone, and R. E. Vogt, Astrophy. J., 201, L95-97, 15 Oct 1975.

"The Isotopic Composition of Hydrogen and Helium in Low Energy Cosmic Rays", R. A. Mewaldt, E. C. Stone, and R. E. Vogt, Ap.J. 206, 616 (1976).

"Observations of Jovian Electrons at 1 AU", R. A. Mewaldt, E. C. Stone, anc R. E. Vogt, JGR, 81, 2397 (1976).

"Isotopic and Elemental Composition of the Anomalous Low Energy Cosmic Ray Fluxes", R. A. Mewaldt, E. C. Stone, S. B. Vidor, and R. E. Vogt, Ap.J.205, 931,(1976).

"Correlation of Electrons $E_e > 0.2$ MeV with Low Energy Electrons (50 eV $\leq E_e \leq 50$ KeV) in the Earth's Magnetotail", D. N. Baker, E. C. Stone, R. E. Vogt, K. L. Ackerson, and L. A. Frank, Fall AGU Mtg, San Francisco, 1975, Trans. Am. Geo. Union, 56, 1046 (1975).

"Neutral Particle Background in Cosmic Ray Telescopes Composed of Silicon Solid State Detectors", R. A. Mewaldt, E. C. Stone, and R. E. Vogt, to be published in Space Science Instrumentation, 1977.

"Energetic Electron Anisotropies in the Magnetotail: Identification of Open and Closed Field Lines", D. N. Baker, and E. C. Stone, Geophys. Res. Letters, 3, 557 (1976).

"Energetic Electrons Observed in Conjunction with Magnetotail Fireball Events", D. N. Baker, E. C. Stone, R. E. Vogt, L. A. Frank, K. L. Ackerson, Trans. Am. Geophys. Union, 57, 314 (1976).

"The Isotopic and Elemental Composition of ~ 4 to ~ 30 MeV/nucleon Cosmic Rays", R. E. Vogt, R. A. Mewaldt, and E. C. Stone, Bull. Am. Phys. Soc., 21, 540 (1976).

"Deuterium and ^{3}He in Low Energy Cosmic Rays", R. A. Mewaldt, E. C. Stone, and R. E. Vogt, ibid, p. 641.

"Quiet Time Measurements of Low Energy Hydrogen and Helium Nuclei: 1972-1975", E. C. Stone, R. A. Mewaldt, and R. E. Vogt, ibid. p. 641.

"Observations of Energetic Electrons (E $\geqslant$ 200 KeV) in the Earth's Magnetotail: Plasma Sheet and Fireball Observations", D. N. Baker, E. C. Stone, J. Geophys. Res. 82, 1537 (1977).

"Persistent Sunward Flow of ~ 1.6 MeV Protons at 1 AU", F. E. Marshall, E. C. Stone, Geophys. Res. Ltrs. 4, 57 (1977).

"The Magnetopause Electron Layer Along the Distant Magnetotail", D. N. Baker and E. C. Stone, ibid, p.133 (1977).

"High Energy Electrons (E $\geqslant$ 200 keV) Observed in the High Magnetotail Boundary Layer", D. N. Baker and E. C. Stone, Trans. Am. Geo. Union, 57, 995 (1976).

"A Steady-State Model of Sunward Flow of Low Energy Protons", E. C.Stone and F. E. Marshall, ibid, p.980 (1976).

"Persistent Sunward Flow of ~ 1.6 MeV Protons at 1 AU", F. E. Marshall and E. C. Stone, ibid, p.980 (1976).

"Observations of 1 to 6 MeV Electrons in 1976", S. R. Hartman, R. A. Mewaldt, E. C. Stone and R. E. Vogt, Tucson Conf. on Solar & Inter-plan. Physics, January 1977.

"The Dependence of Sunward Streaming on the Interplanetary Magnetic Field", F. E. Marshall and E. C. Stone, ibid, 1977.

"Characteristics of α Particles During Periods of Moderately Enhanced Proton Fluxes", ibid, 1977.

"A Comparative Study of the Solar Modulation of the Anomalous Low Energy Cosmic Rays", ibid, 1977.

"The Magnetopause Energetic Electron Layer 1, Observations Along the Distant Magnetotail", D. N. Baker and E. C. Stone, to be submitted to J. Geophys. Res.

"Thickness and Intensity Characteristics of the Tailward Magnetopause Energetic Electron Layer", D. N. Baker and E. C. Stone, Trans. Am. Geo. Union, 58, 471, (1977)

"Observations of Electron Acceleration and Closed Field LInes in Magnetosheath-like Regions", E. C. Stone and D. N. Baker, ibid, p.471, (1977).

"Energetic Proton Penetration into the Earth's Magnetotail at ~ 30 R_E", R. A. Mewaldt, D. N. Baker, and E. C. Stone, ibid, p.475 (1977).

"Characteristics of Sunward Flowing Proton and Alpha Particle Fluxes of Moderate Intensity", F. E. Marshall and E. C.Stone, submitted to J.Geophys. Res. October 1977.

"The Relationship of Energy Flow at the Magnetopause to Geomagnetic Activity", D. N. Baker and E. C. Stone, Geophys. Res. Letters 4, 395, (1977).

"The Magnetopause Electron Layer, 2, Relationship to Geomagnetic Activity", D. N. Baker, and E. C. Stone, to be submitted to J.Geophys. Res. 1977.

"Radial Development of a Solar Cosmic Ray Event Between 0.4 and 1 AU on March 3, 1975 as Observed From Helios 1 and IMP-7", G. Wibberenz, H. Kunow, G. Green, R. Müller-Mellin, M. Witte, H. Hempe, R. A. Mewaldt, E. C. Stone, R. E. Vogt and R. Reinhard, 15th Int'l. Cosmic Ray Conference, Plovdiv, Bulgaria, Conf. Papers, 5, 188 (1977).

"Persistent Sunward Flow of ~ 1.6 MeV Protons at 1 AU", F. E. Marshall and E. C. Stone, ibid, 5, 197 (1977).

"Deuterium and ^{3}He in Low Energy Cosmic Rays", R. A. Mewaldt, E. C. Stone, and R. E. Vogt, ibid 2, 321 (1977).

Isotopic and Elemental Composition of Cosmic Rays Below ~ 30 MeV/nuc", R. A. Mewaldt, E. C. Stone, and R. E. Vogt, ibid, 2, 323 (1977).

"Temporal Variations in the Composition of Low Energy Cosmic Rays", R. A. Mewaldt, E. C. Stone and R. E. Vogt, ibid 2, 322 (1977).

"Simultaneous Observations of Cosmic Ray Particles in Corotating Interplanetary Structures at Different Solar Distances Between 0.3 and 1.0 AU from HELIOS 1 and 2 and IMP 7 and 8", H. Kunow, G. Wibberenz, G. Green, R. Müller-Mellin, R. Witte, E. Hempe, E. C. Stone, R. A. Mewaldt, and R. E. Vogt, ibid, Vol. 3 (1977).

LIST OF TABLES

1 NOMINAL DETECTOR PROPERTIES FOR IMP-7 EIS

2 PROPERTIES OF VARIOUS MODES OF OPERATION FOR IMP-7 EIS

3 NOMINAL DISCRIMINATOR THRESHOLDS FOR IMP-7 EIS

4 NOMINAL DETECTOR PROPERTIES FOR IMP-8 EIS

5 PROPERTIES OF VARIOUS MODES OF OPERATION FOR IMP-8 EIS

6 PROPERTIES OF VARIOUS IMP-7 EIS RATES

7 PROPERTIES OF VARIOUS IMP-8 EIS RATES

8 TAPE FORMAT

TABLE 1 - NOMINAL DETECTOR PROPERTIES FOR IMP-7 EIS

Detector	Type	Thickness (μm)	Outer Dia. (mm)	Inner Dia. (mm)
D0, D1, D3	Annular	1000	22	8
D4	Annular	1000	25	8
D2	Solid	50	9	-
D5-D10	Solid	1000	21	-

TABLE 2 - PROPERTIES OF VARIOUS MODES OF OPERATION FOR IMP-7 EIS

MODE	LOGIC REQUIREMENTS	POSSIBLE EVENT RANGES	PARTICLE TYPE	ENERGY RANGE (MeV)	GEOMETRICAL FACTOR (cm^2sr)
Narrow Geometry = (D2 + D5)·N·S	$\overline{d2}\cdot\underline{D5}\cdot\overline{d5h}\cdot N\cdot S$	D5 to D9	e	0.2 to ~ 4	~ 0.05+
	$D2\cdot\overline{d5}\cdot N\cdot S$	D2	p	1.2 to 2.4	0.2
	$(D2\cdot D5 + D5H)\cdot N\cdot S$	D5 to D9	p	2.4 to 31	0.07
Wide Geometry = D0·S	D0·S	D0 to D9	e	0.16 to ~ 6	~ 2.4+
			p	1.1 to 43	1.8 to 0.3*
Neutral Mode = $D7\cdot\overline{d5}\cdot N\cdot S$	$D7\cdot\overline{d5}\cdot N\cdot S$	D6 to D9	γ, n	...	...

NOTES:

$\overline{dn}$ denotes "not" DN.

N = "narrow" = $\overline{d0}\cdot\overline{d1}\cdot\overline{d2}\cdot\overline{d3}$

S = "stopping" = $d\overline{10}\cdot\overline{d11}$

D5H = 3.0 MeV (high) threshold of D5

Modes triggered by protons can, of course, also be triggered by heavier nuclei of appropriate energies.

Electron threshold energies cannot be sharply defined because of scattering effects.

+Electron geometry factors are somewhat energy dependent. Geometry factors for electrons are somewhat larger than for protons because of electron events that scatter from the inside of the D11 housing.

*Depending on particle range.

TABLE 3 - NOMINAL DISCRIMINATOR THRESHOLDS FOR IMP-7 EIS

DETECTOR	THRESHOLDS
D0, D1, D3 D4, D6-D10	160 KeV
D2	160 KeV
D2H	400 KeV
D5	160 KeV
D5H	3 MeV

TABLE 4 - NOMINAL DETECTOR PROPERTIES FOR IMP-8 EIS

Detector	Type	Thickness (μm)	Outer Dia. (mm)	Inner Dia. (mm)
D0	Annular	1000	22	8
D1	Annular	1000	23	8
D2	Solid	50	9	
D3-5, 7, 9, 10	Solid	1000	22	
D6, D8	Solid	1000	23	

TABLE 5 - PROPERTIES OF VARIOUS MODES OF OPERATION FOR IMP-8 EIS

Mode(+)	Possible Event Ranges	Particle Type	Energy Range (MeV)	Geometrical Factor ($cm^2 sr$)
Narrow	D5 to D8	e	0.2 to ~ 4	~ 0.2 +
	D2	p	1.3 to 2.5	0.23
	D5 to D8	p	2.5 to 27	0.23
Wide	D0 to D9	e	0.16 to ~ 6	~ 1.8+
		p	1.3 to 43	1.1 to 0.4*
Neutral	D6 to D8	n,γ	...	...

(+) Logic requirements are the same as in Table 2.

\+ Electron geometry factors are somewhat energy dependent.

* Depending on particle range.

See notes for Table 2.

TABLE 6 - PROPERTIES OF VARIOUS IMP-7 EIS RATES

Rate Name	Logic Requirements (#)	Particle Type	Energy Range (MeV)	Background Counts/sec*	Geometrical Factor ($cm^2 sr$)	Comment
ELO	$N \cdot S \cdot \overline{d2h} \cdot D5 \cdot \overline{d5h} \cdot \overline{d6} \cdot \overline{d7} \cdot \overline{b}$	e	0.2 to ~ 1	~ 0.05	~ 0.05+	
EHI	$N \cdot S \cdot \overline{d2} \cdot D5 \cdot \overline{d5h} \cdot D6$	e	~ 1 to ~ 5	~ 0.02	~ 0.07+	
PLO	$N \cdot S \cdot D2H \cdot \overline{d5} \cdot \overline{d5h} \cdot \overline{d6} \cdot \overline{d7} \cdot \overline{b}$	p	1.2 to 2.4	$\leq 3 \times 10^{-4}$	0.07	
PHI	$N \cdot S \cdot D2 \cdot D5H \cdot \overline{d6}$	p	4 to ~ 10	$\leq 10^{-5}$	0.07	
DO*	$DO \cdot S$	e p	~0.16 to ~6 1 to 43	~ 0.1	~ 2.4+ 1.8	
DO1*	$DO \cdot D1 \cdot S$	e p	~ 1 to ~ 6 12.5 to 43	~ 0.02	~ 1.6+ 1.4	Mostly e at quiet times
PEN	$N \cdot D5 \cdot D6 \cdot D10 \cdot \overline{d11}$	p	≥ 30	~ 0.02	0.03	Also includes particles moving "backwards".
NEUT	$N \cdot S \cdot \overline{d5} \cdot D7$	γ,n	...	~ 0.09	...	Mostly gamma rays.

(#) B = "busy". See also notes for Table 2.

* All background rates may vary by about ±10%, depending on the integral flux of high energy cosmic rays. Variations of this type scale with the NEUT rate.

\+ Electron geometry factors are somewhat energy dependent. See also Section IV-D.

TABLE 7 - PROPERTIES OF VARIOUS IMP-8 EIS RATES

Rate Name	Particle Type	Energy Range (MeV)	Background Counts/sec*	Geometrical Factor ($cm^2 sr$)	Comment
ELO	e	~0.2 to ~ 1	~ 0.05	~ 0.2 +	
EHI	e	~ 1 to ~ 4	~ 0.02	~ 0.2 +	
PLO	p	1.3 to 2.5	$\leq 3 \times 10^{-4}$	0.23	
PHI	p	4 to 13	$\leq 10^{-5}$	0.23	
DO*	e p	~0.16 to ~6 1 to 43	~ 0.1	~ 1.8+ 1.1	
DO1*	e p	~ 1 to ~ 6 12.5 to 43	~ 0.02	~ 1.5+ 1.0	Mostly e at quiet times.
PEN	...	...	$< 10^{-4}$	...	Not generally useful.
NEUT	γ,n	...	~ 0.08	...	Mostly gamma rays.

Notes:

See also notes for Table 2. See Table 6 for logic requirements.

* All background rates may vary by about ±10%, depending on the integral flux of high energy cosmic rays. Variations of this type scale with the NEUT rate.

\+ Somewhat energy dependent.

TABLE 8

TAPE FORMAT

Item No.	Data Type	Mnemonic	Description and Comments
1	I	IFN	File Number, from 1 to 37 10 days per file
2	I	IRN	Record Number, from 1 to 240 1 hour per record
3	I	IDSAT	Satellite Identification 7 or -7 → IMP-7 = IMP-H 8 or -8 → IMP-8 = IMP-J negative → no data this hour
4	I	IYR	Year, from 72 up
5	I	IDY	Day, from 1 to 366
6	I	IHR	Hour, from 1 to 24
7	I	ITIME	Time, from 7200101 up ITIME = IHR + 100* IDY + 100000* IYR
8-10	-		Spare
11	I	KNT(1)	Event count, D2 protons, 1.43-2.34 MeV
12	I	KNT(2)	Event count, D25 protons, 2.5-4.0 MeV
13	I	KNT(3)	Event count, D25 protons, 4.0-7.0 MeV
14	I	KNT(4)	Event count, D25 protons, 7.0-12.5 MeV
15	I	KNT(5)	Event count, D2 alphas, 1.43-2.34 MeV/nuc
16	I	KNT(6)	Event count, D25 alphas, 2.5-4.0 MeV/nuc
17	I	KNT(7)	Event count, D25 alphas, 4.0-7.0 MeV/nuc
18	I	KNT(8)	Event count, D25 alphas, 7.0-12.5 MeV/nuc
19	I	KNT(9)	Event count, D01* electrons, ~ 1-5 MeV
20	-		Spare
21	I	IR(1)	D0* rate in units of counts per day
22	I	IR(2)	D01* rate in units of counts per day
23	I	IR(3)	ELO rate in units of counts per day
24	I	IR(4)	EHI rate in units of counts per day
25	I	IR(5)	PLO rate in units of counts per day
26	I	IR(6)	PHI rate in units of counts per day
27	I	IR(7)	PEN rate in units of counts per day
28	I	IR(8)	NEUT rate in units of counts per day
29	I	IR(9)	D0 rate in units of counts per day
30	I	IR(10)	D1 rate in units of counts per day
31	I	IR(11)	D2 rate in units of counts per day
32	I	IR(12)	D3 rate in units of counts per day
33	I	IR(13)	D4 rate in units of counts per day
34	I	IR(14)	D5 rate in units of counts per day
35	I	IR(15)	D6 rate in units of counts per day

Item No.	Data Type	Mnemonic	Description and Comments
36	I	IR(16)	D7 rate in units of counts per day
37	I	IR(17)	D8 rate in units of counts per day
38	I	IR(18)	D9 rate in units of counts per day
39	I	IR(19)	D10 rate in units of counts per day
40	I	IR(20)	•D11 rate in units of counts per day
41	I	IRU(1)	Uncertainty in DO* rate in units of counts per day
42	I	IRU(2)	Uncertainty in DO1* rate in units of counts per day
43	I	IRU(3)	Uncertainty in ELO rate in units of counts per
44	I	IRU(4)	Uncertainty in EHI rate in units of counts per day
45	I	IRU(5)	Uncertainty in PLO rate in units of counts per day
46	I	IRU(6)	Uncertainty in PHI rate in units of counts per day
47	I	IRU(7)	Uncertainty in PEN rate in units of counts per day
48	I	IRU(8)	Uncertainty in NEUT rate in units of counts per day
49	I	IRU(9)	Uncertainty in DO rate in units of counts per day
50	I	IRU(10)	Uncertainty in D1 rate in units of counts per day
51	I	IRU(11)	Uncertainty in D2 rate in units of counts per day
52	I	IRU(12)	Uncertainty in D3 rate in units of counts per day
53	I	IRU(13)	Uncertainty in D4 rate in units of counts per day
54	I	IRU(14)	Uncertainty in D5 rate in units of counts per day
55	I	IRU(15)	Uncertainty in D6 rate in units of counts per day
56	I	IRU(16)	Uncertainty in D7 rate in units of counts per day
57	I	IRU(17)	Uncertainty in D8 rate in units of counts per day
58	I	IRU(18)	Uncertainty in D9 rate in units of counts per day
59	I	IRU(19)	Uncertainty in D10 rate in units of counts per day
60	I	IRU(20)	Uncertainty in D11 rate in units of counts per day

Item No.	Data Type	Mnemonic	Description and Comments
61	-	LTNG	Spare
62	I	LTNG	Narrow geometry live time in sec
63	I	LTWG	Wide geometry live time in sec
64-7	-		Spare
68	R	TLNG	Narrow geometry live time in sec
69	R	TLWG	Wide geometry live time in sec
70	-		Spare
71	R	FLX(1)	Flux, D2 protons, 1.43-2.34 MeV
72	R	FLX(2)	Flux, D25 protons, 2.5-4.0 MeV
73	R	FLX(3)	Flux, D25 protons, 4.0-7.0 MeV
74	R	FLX(4)	Flux, D25 protons, 7.0-12.5 MeV
75	R	FLX(5)	Flux, D2 alphas, 1.43-2.34 MeV/nuc
76	R	FLX(6)	Flux, D25 alphas, 2.5-4.0 MeV/nuc
77	R	FLX(7)	Flux, D25 alphas, 4.0-7.0 MeV/nuc
78	R	FLX(8)	Flux, D25 alphas, 7.0-12.5 MeV/nuc
79	R	FLX(9)	Flux, DO1* electrons, ~ 1 to 5 MeV
80	-		Spare
81	R	UFLX(1)	Uncertainty in flux, D2 protons, 1.43-2.34 MeV
82	R	UFLX(2)	Uncertainty in flux, D25 protons, 2.5-4.0 MeV
83	R	UFLX(3)	Uncertainty in flux, D25 protons, 4.0-7.0 MeV
84	R	UFLX(4)	Uncertainty in flux, D25 protons, 7.0-12.5 MeV
85	R	UFLX(5)	Uncertainty in flux, D2 alphas, 1.43-2.34 MeV/nuc
86	R	UFLX(6)	Uncertainty in flux, D25 alphas, 2.5-4.0 MeV/nuc
87	R	UFLX(7)	Uncertainty in flux, D25 alphas, 4.0-7.0 MeV/nuc
88	R	UFLX(8)	Uncertainty in flux, D25 alphas, 7.0-12.5 MeV/nuc
89	R	UFLX(9)	Uncertainty in flux, DO1* electrons, ~ 1-5 MeV
90	-		Spare
91	R	R(1)	DO* rate in counts per second
92	R	R(2)	DO1* rate in counts per second
93	R	R(3)	ELO rate in counts per second
94	R	R(4)	EHI rate in counts per second
95	R	R(5)	PLO rate in counts per second

Item No.	Data Type	Mnemonic	Description and Comments
96	R	R(6)	PHI rate in counts per second
97	R	R(7)	PEN rate in counts per second
98	R	R(8)	NEUT rate in counts per second
99	R	R(9)	D0 rate in counts per second
100	R	R(10)	D1 rate in counts per second
101	R	R(11)	D2 rate in counts per second
102	R	R(12)	D3 rate in counts per second
103	R	R(13)	D4 rate in counts per second
104	R	R(14)	D5 rate in counts per second
105	R	R(15)	D6 rate in counts per second
106	R	R(16)	D7 rate in counts per second
107	R	R(17)	D8 rate in counts per second
108	R	R(18)	D9 rate in counts per second
109	R	R(19)	D10 rate in counts per second
110	R	R(20)	D11 rate in counts per second
111	R	RU(1)	Uncertainty in D0* rate in counts per second
112	R	RU(2)	Uncertainty in D01* rate in counts per second
113	R	RU(3)	Uncertainty in ELO rate in counts per second
114	R	RU(4)	Uncertainty in EHI rate in counts per second
115	R	RU(5)	Uncertainty in PLO rate in counts per second
116	R	RU(6)	Uncertainty in PHI rate in counts per second
117	R	RU(7)	Uncertainty in PEN rate in counts per second
118	R	RU(8)	Uncertainty in NEUT rate in counts per second
119	R	RU(9)	Uncertainty in D0 rate in counts per second
120	R	RU(10)	Uncertainty in D1 rate in counts per second
121	R	RU(11)	Uncertainty in D2 rate in counts per second
122	R	RU(12)	Uncertainty in D3 rate in counts per second
123	R	RU(13)	Uncertainty in D4 rate in counts per second
124	R	RU(14)	Uncertainty in D5 rate in counts per second
125	R	RU(15)	Uncertainty in D6 rate in counts per second
126	R	RU(16)	Uncertainty in D7 rate in counts per second

Item No.	Data Type	Mnemonic	Description and Comments
127	R	RU(17)	Uncertainty in D8 rate in counts per second
128	R	RU(18)	Uncertainty in D9 rate in counts per second
129	R	RU(19)	Uncertainty in D10 rate in counts per second
130	R	RU(20)	Uncertainty in D11 rate in counts per second

Figure 1a - Schematic of the IMP-7 EIS. Detectors D0 through D10 are 1 mm thick silicon surface-barrier detectors, except D2 which is 50 microns thick. D0, D1, D3, and D4 are annular devices. D11 is a plastic scintillator anticoincidence cup viewed by a photomultiplier tube.

Figure 1b - Schematic of the IMP-8 EIS. Detectors D0 through D10 are 1 mm thick silicon surface-barrier detectors, except D2 which is 50 microns thick. D0 and D1 are annular devices. D11 is a plastic scintillator anticoincidence cup.

Figure 2 - Singles rates for a period of about 7-$^1/_2$ days beginning on day 101 of 1973 (Figure 2a) and singles rates for a period of about 28 days beginning on day 92 or 1973 (Figure 2b). The spike in several of the rates on the major grid mark preceding day 108 is clearly an artifact. Although it is barely visible on this logarithmic scale, D7 was slightly noisy around DAY 95 and was turned off for about 5 days. This action causes a gap in the D7 singles rate curve on Figure 2b and the NEUT rate on Figure 3b (distinct from the data gap around DAY 101).

The depression in the single detector rates (D6 - D9) visible on DAYS 103-105 of Figure 2b is the result of a Forbush decrease.

Figure 3 - Orbit parameters and coincidence rates are shown for the same periods as in Figure 2. The features of Figure 3b are a solar flare on day 102 and a magnetotail passage centered on day 112. Note that the tail passage is indicated by the SES ANGLE. A somewhat smaller flare is

visible on day 114.

From inspection of the ELO, PLO, and DO* rates, and the information in Table 6, it can be seen that protons dominate the DO* rate during days 102-109. On the other hand, during days 110-118, DO* is dominated by electrons associated with the magnetospheric tail. Qualitative information on the electron and proton energy spectra can be obtained from comparison of the ELO and EHI, and PLO and PHI rates.

Figure 4 - Calibration results for IMP-7 ELO and EHI rates. See section IV.C for description.

Figure 5 - Calibration results for IMP-8 ELO and EHI rates. See section IV.C for description.

Figure 6 - Response of the IMP-7 DO* and DO1* rates to electrons. See section IV.D.

Figure 7 - Response of the IMP-8 DO* and DO1* rates to electrons. See section IV.D.

Figure 8 - Alpha particle contamination of D2 proton fluxes as a function of the spectral index γ. See section V.C.

IMP-7
CALTECH ELECTRON/ISOTOPE SPECTROMETER

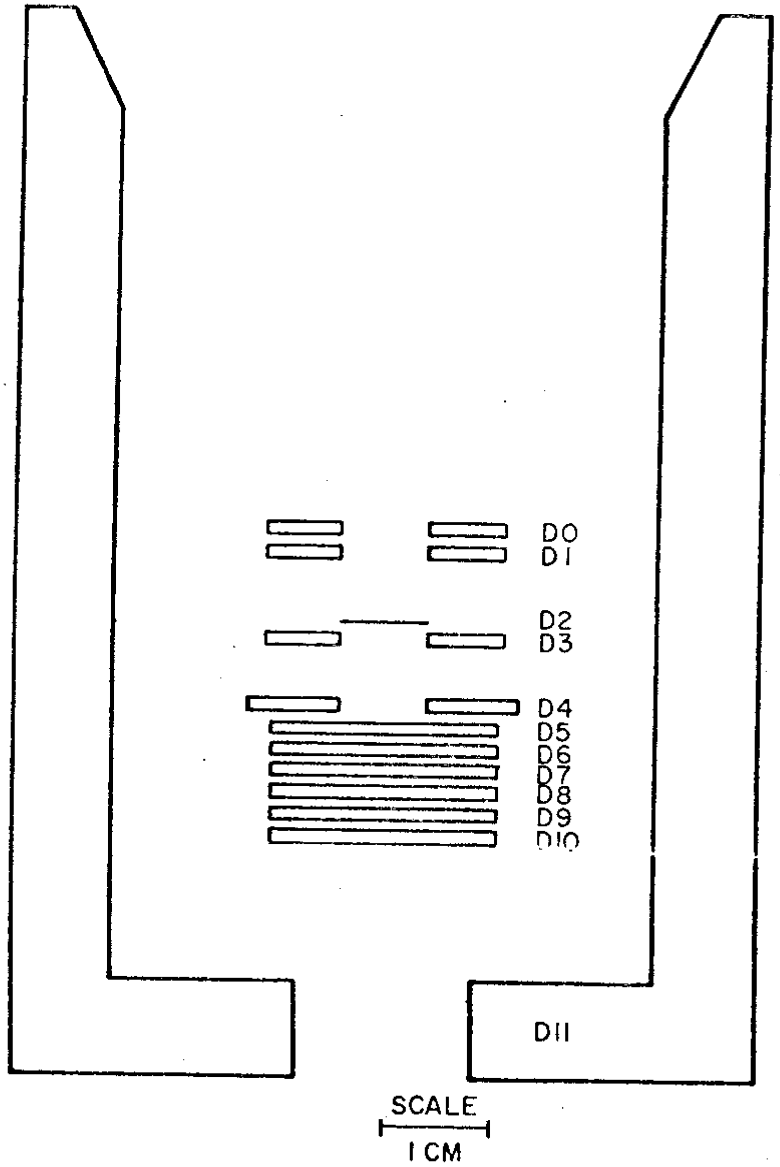

Figure 1a

IMP-8
CALTECH ELECTRON/ISOTOPE SPECTROMETER

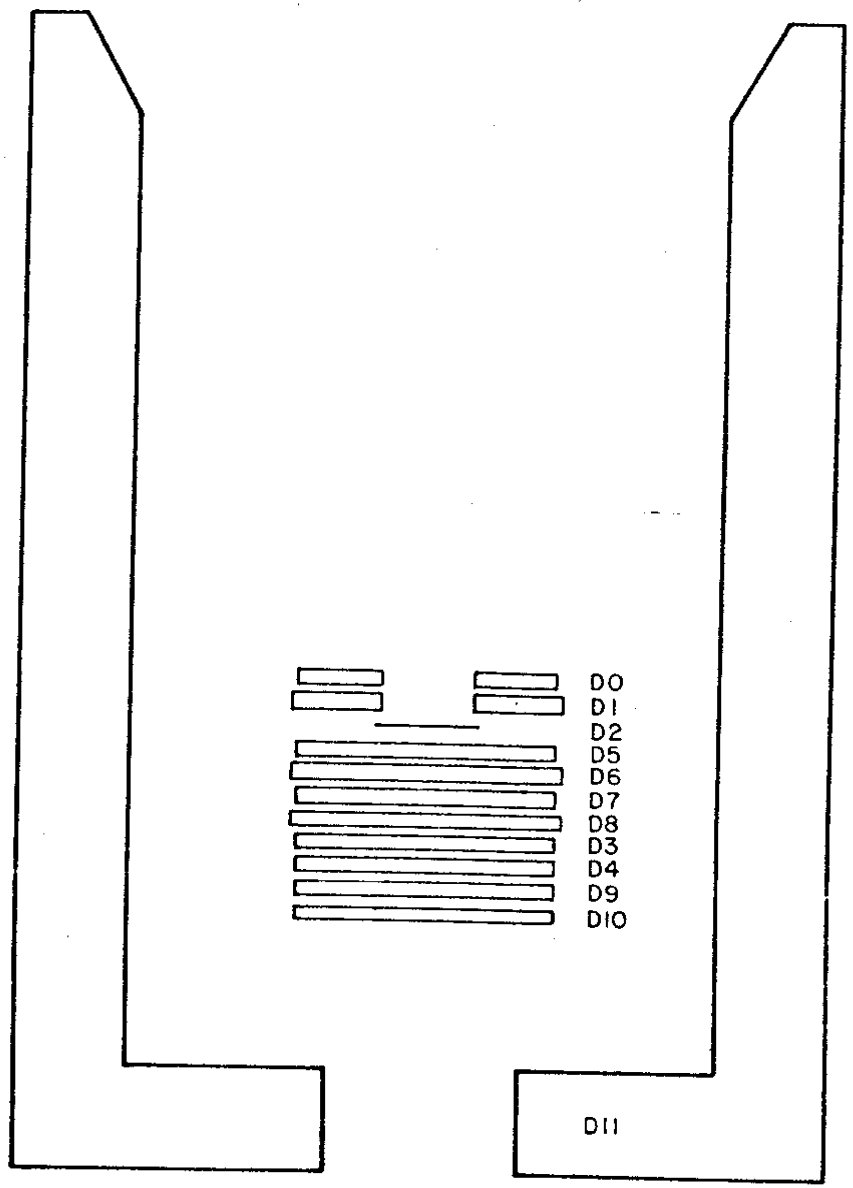

Figure 1b

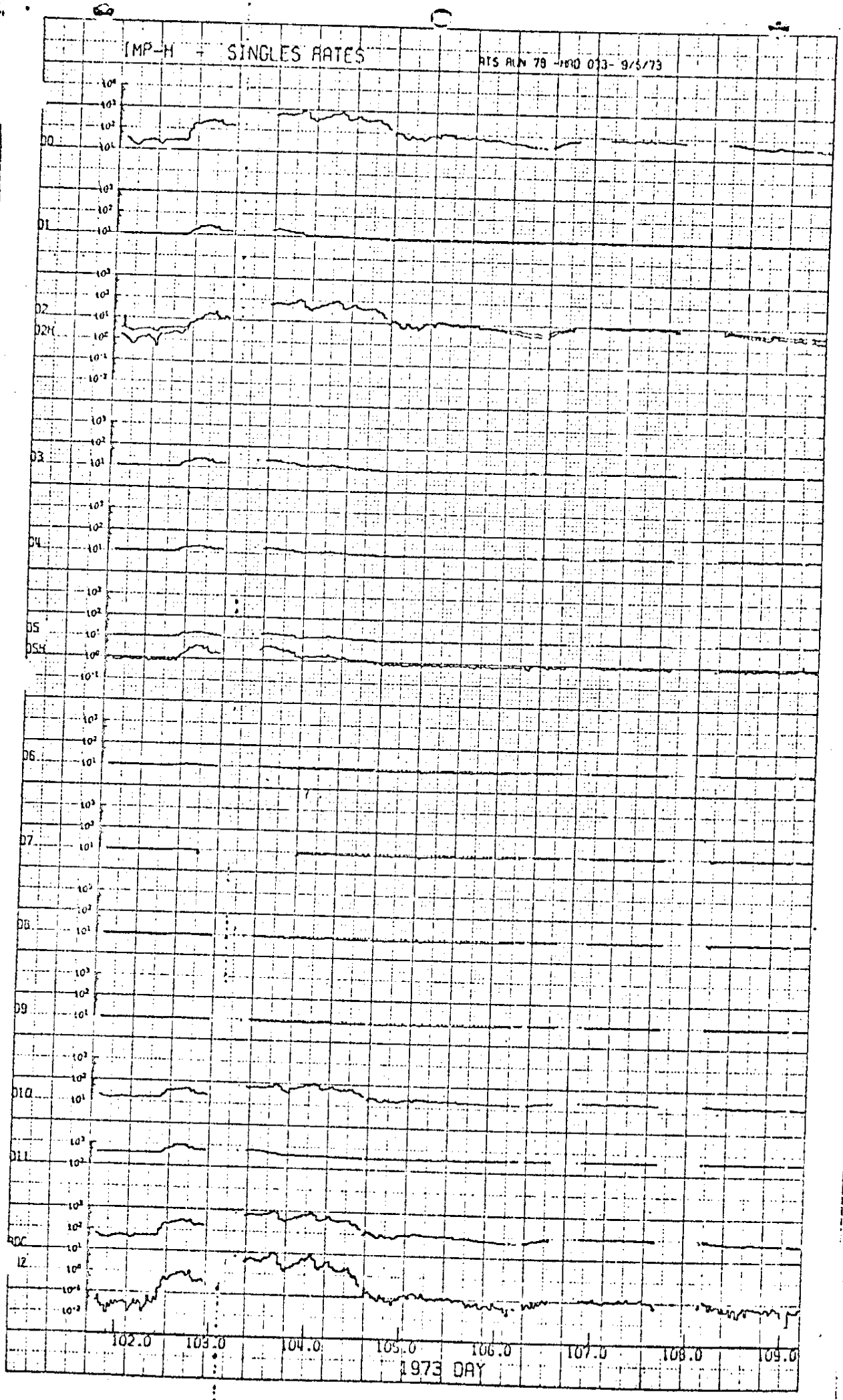
IMP-H - SINGLES RATES
RTS RUN 78 -HRD 073- 9/5/73
D0
D1
D2
D2H
D3
D4
D5
D5H
D6
D7
D8
D9
D10
D11
ADC
I2
102.0
103.0
104.0
105.0
106.0
107.0
108.0
109.0
1973 DAY

Figure 2a

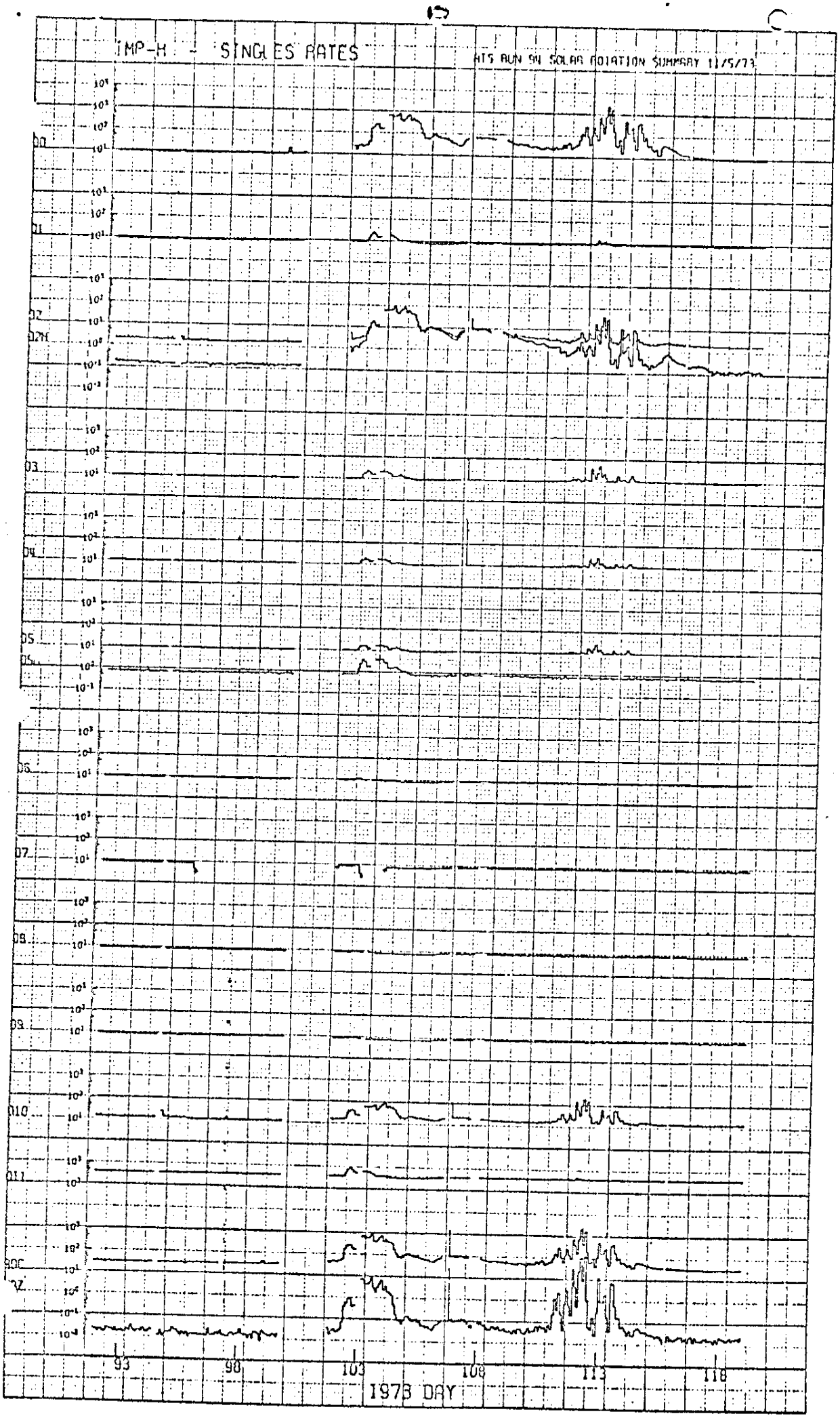
IMP-H - SINGLES RATES
HTS RUN 94 SOLAR ROTATION SUMMARY 11/5/73
93
98
103
108
113
118
1973 DAY

Figure 2b

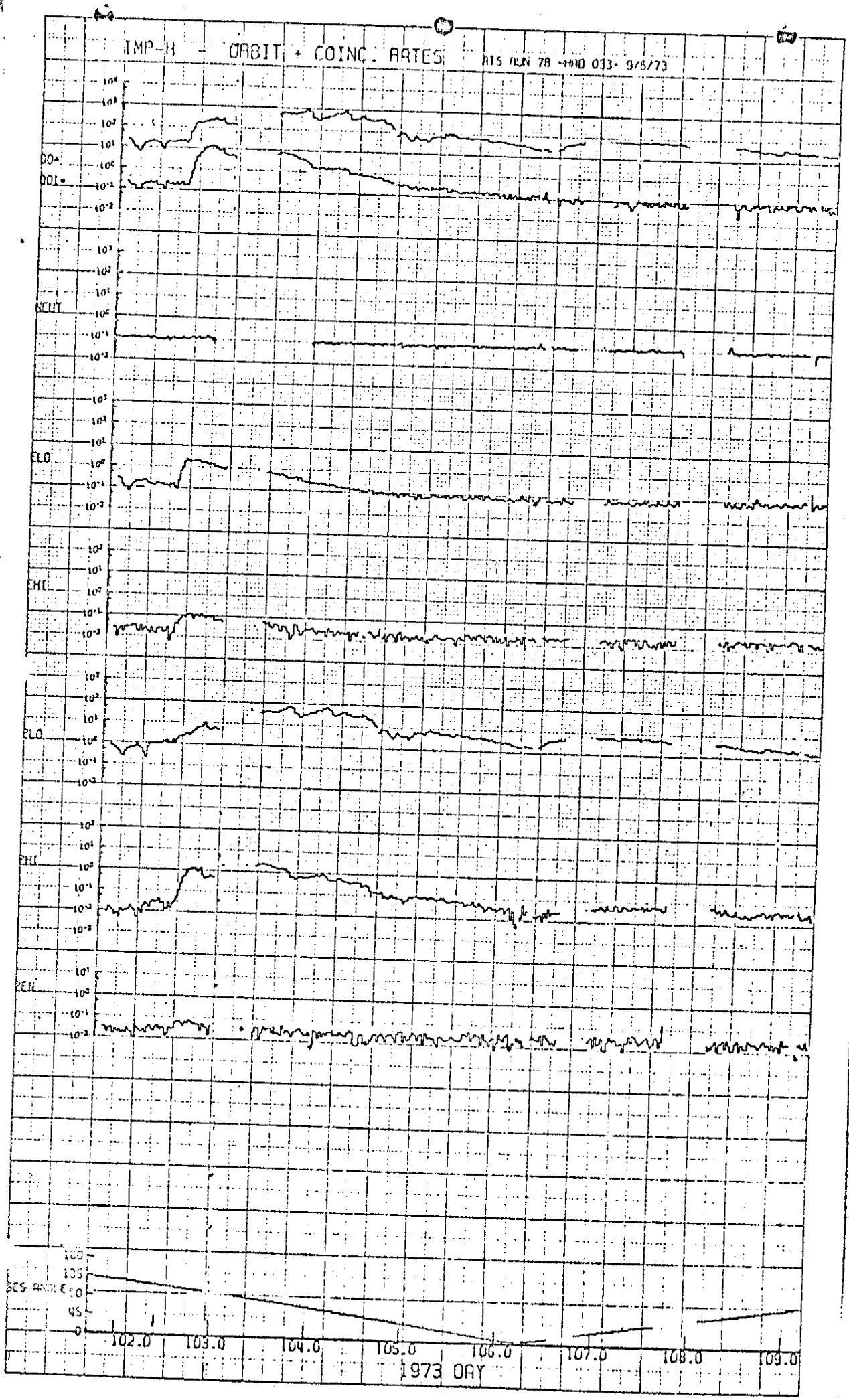
IMP-H - ORBIT + COINC. RATES
RTS RUN 78 -HAD 033- 9/6/73
DO
DOI
NEUT
ELO
EHI
PLO
PHI
PEN
SES ANGLE
102.0
103.0
104.0
105.0
106.0
107.0
108.0
109.0
1973 DAY

Figure 3a

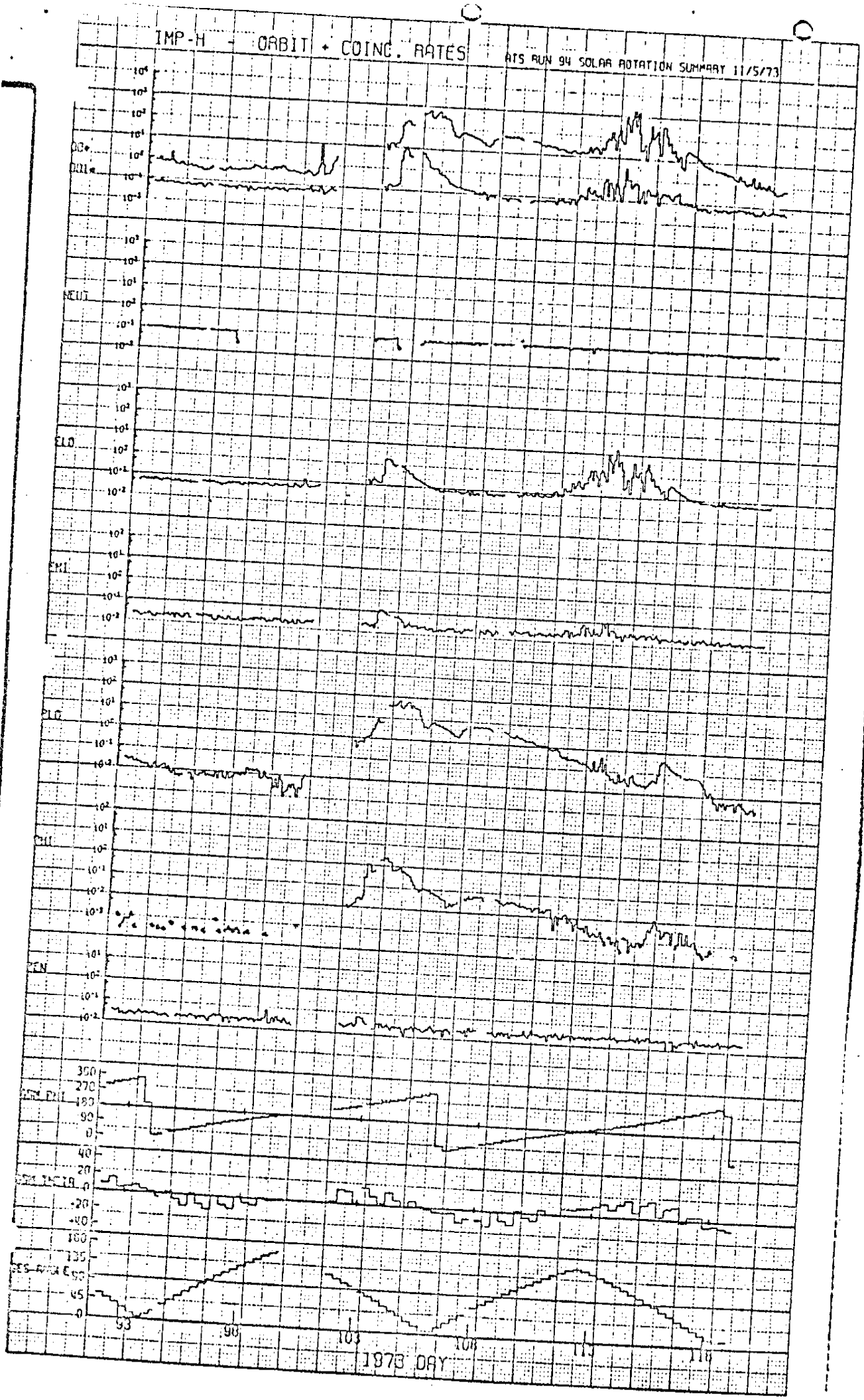
IMP-H - ORBIT + COINC. RATES
ATS RUN 94 SOLAR ROTATION SUMMARY 11/5/73
1973 DAY

Figure 3b

FIGURE 4

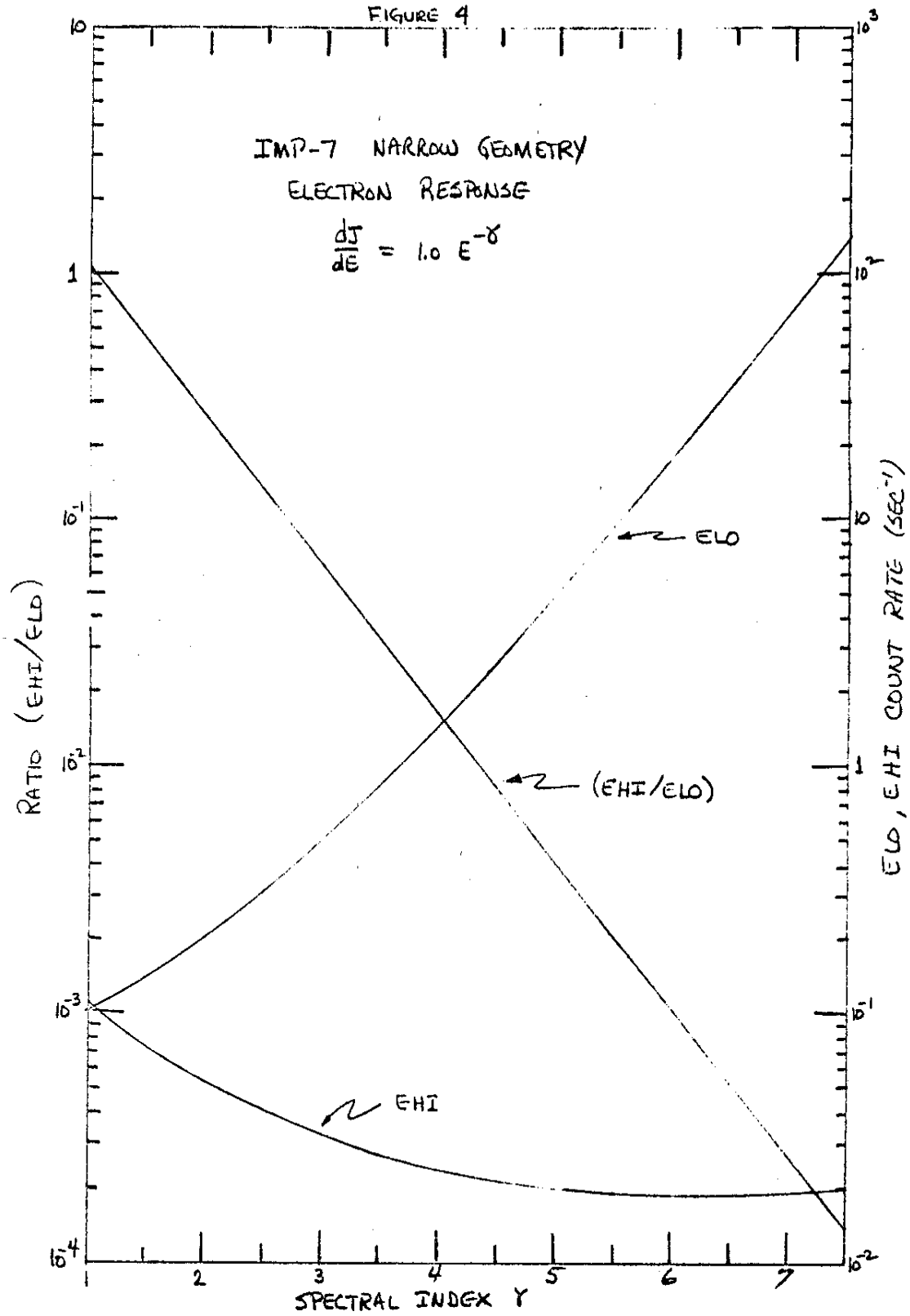
IMP-7 NARROW GEOMETRY
ELECTRON RESPONSE
$\frac{dJ}{dE} = 1.0\ E^{-\gamma}$
ELO
(EHI/ELO)
EHI
RATIO (EHI/ELO)
ELO, EHI COUNT RATE (SEC^{-1})
SPECTRAL INDEX γ
10
1
10^{-1}
10^{-2}
10^{-3}
10^{-4}
10^{3}
10^{2}
10
1
10^{-1}
10^{-2}
1
2
3
4
5
6
7

FIGURE 5

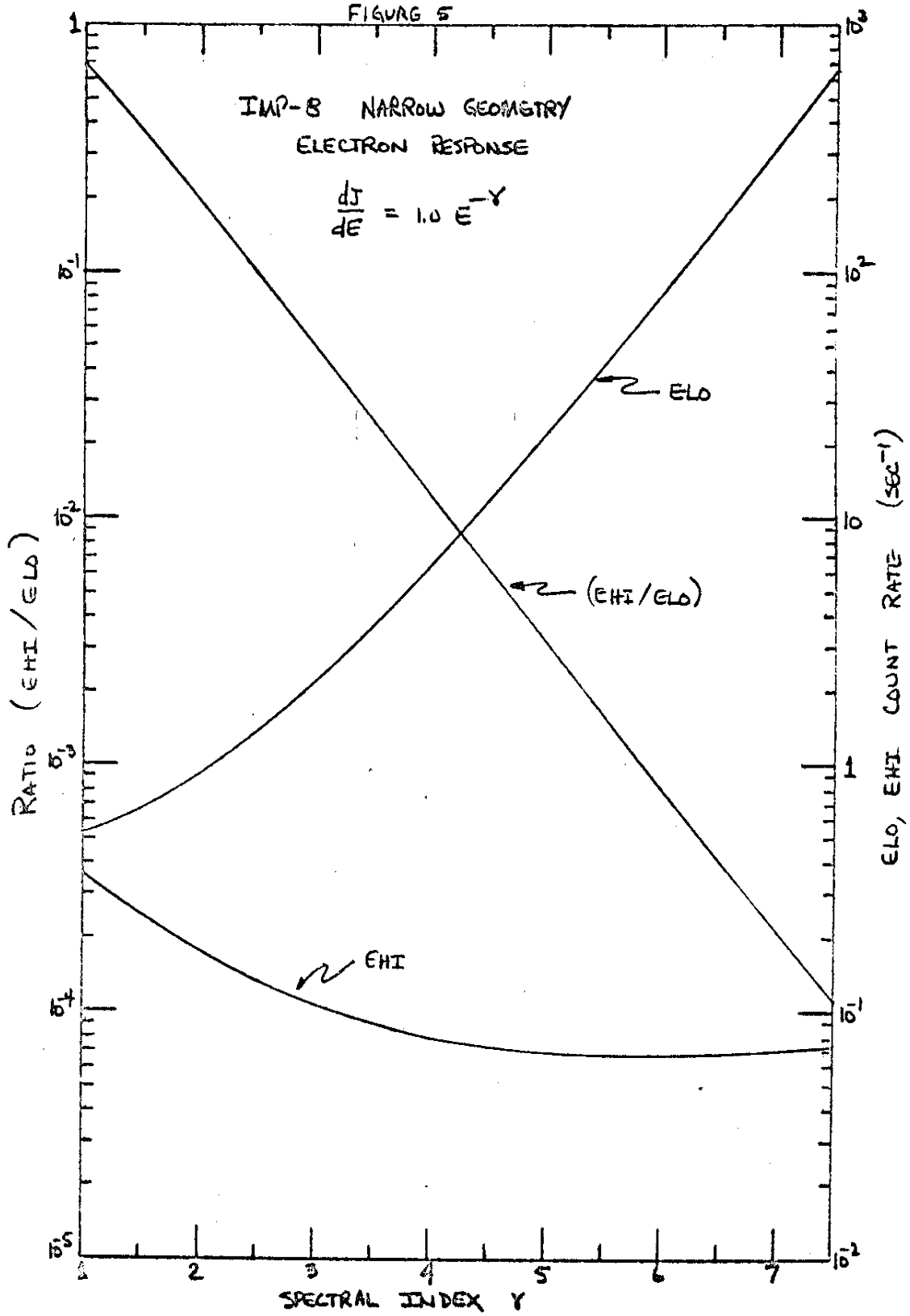
IMP-8 NARROW GEOMETRY
ELECTRON RESPONSE
$\frac{dJ}{dE} = 1.0\ E^{-\gamma}$
ELO
(EHI/ELO)
EHI
RATIO (EHI/ELO)
ELO, EHI COUNT RATE (SEC^{-1})
SPECTRAL INDEX γ
1
10^{-1}
10^{-2}
10^{-3}
10^{-4}
10^{-5}
10^{3}
10^{2}
10
1
10^{-1}
10^{-2}
1
2
3
4
5
6
7

FIGURE 6

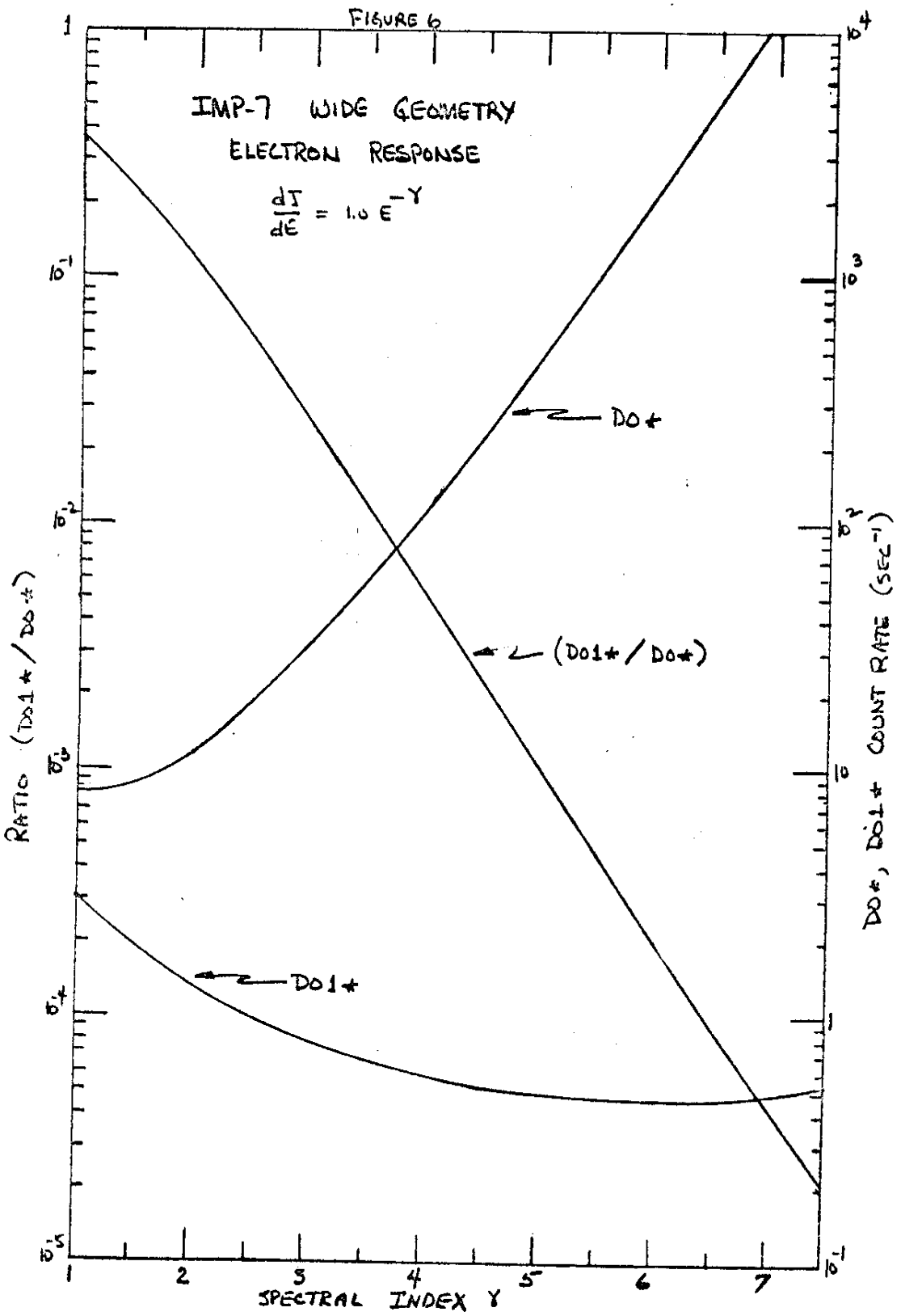
IMP-7 WIDE GEOMETRY
ELECTRON RESPONSE
$\frac{dJ}{dE} = 1.0\ E^{-Y}$
DO+
(DO1+ / DO+)
DO1+
RATIO (DO1+ / DO+)
DO+, DO1+ COUNT RATE (SEC^{-1})
SPECTRAL INDEX Y
1
10^{-1}
10^{-2}
10^{-3}
10^{-4}
10^{-5}
10^{4}
10^{3}
10^{2}
10
1
10^{-1}
1
2
3
4
5
6
7

FIGURE 7

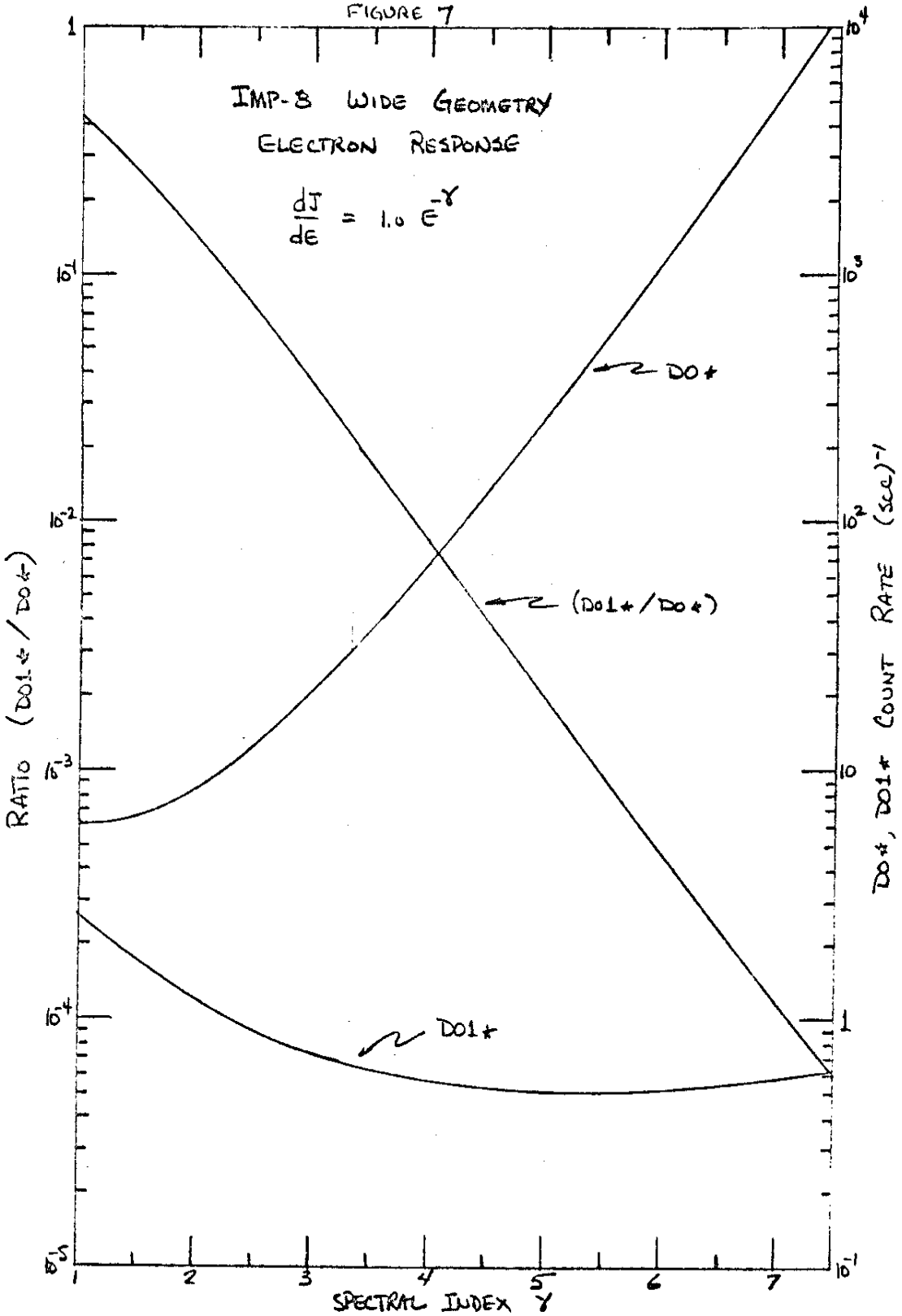
IMP-8 WIDE GEOMETRY
ELECTRON RESPONSE
$\frac{dJ}{dE} = 1.0\ E^{-\gamma}$
DO*
(DO1*/DO*)
DO1*
RATIO (DO1*/DO*)
DO*, DO1* COUNT RATE (SEC)$^{-1}$
SPECTRAL INDEX γ
1
10^{-1}
10^{-2}
10^{-3}
10^{-4}
10^{-5}
10^{4}
10^{3}
10^{2}
10
1
10^{-1}
1
2
3
4
5
6
7

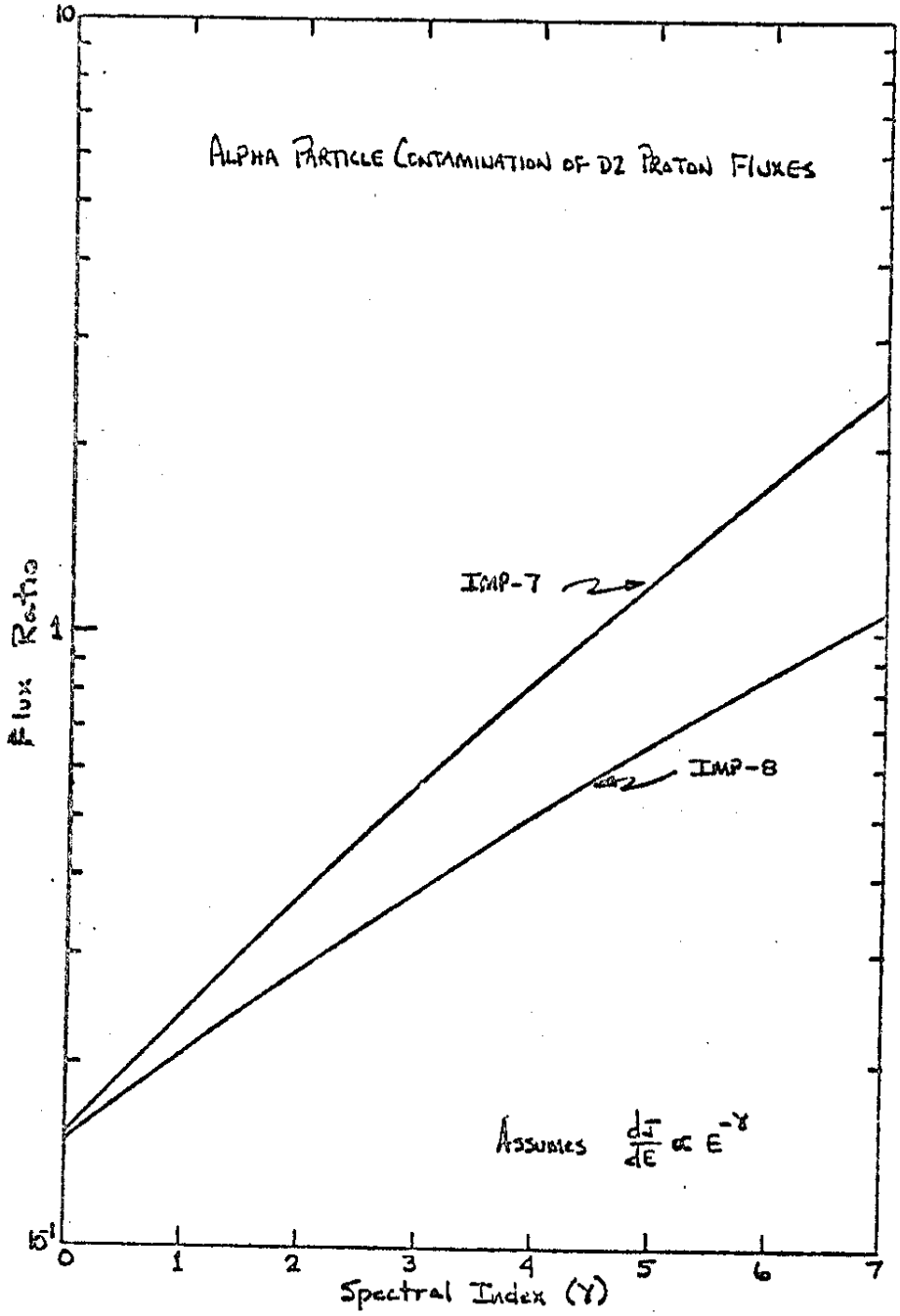

Figure 8 - Alpha particle contamination of D2 proton fluxes. See section V.C for explanation.

CALTECH ELECTRON/ISOTOPE SPECTROMETER

December 1982

"Observations of 0.16 to 3 MeV Electrons during Solar Quiet Times", G. J. Hurford, R. A. Mewaldt, E. C. Stone, and R. E. Vogt, Bull. Am. Phys. Soc., 18, 568 (1973).

"Observations of the Ratio of Low-Energy Cosmic Ray Positrons and Electrons", G. J. Hurford, R. A. Mewaldt, E. C. Stone, and R. E. Vogt, Bull. Am. Phys. Soc., 18, 569 (1973).

"The Energy Spectrum of 0.16 to 3 MeV Electrons during Solar Quiet Times", G. J. Hurford, R. A. Mewaldt, E. C. Stone, and R. E. Vogt, Conf. Papers, 13th Int'l Cosmic Ray Conference, Denver, 1, 324 (1973).

"Observations of the Ratio of Low-Energy Cosmic Ray Positrons and Electrons during Solar Quiet Times", G. J. Hurford, R. A. Mewaldt, E. C. Stone, and R. E. Vogt, Conf. Papers, 13th Int'l Cosmic Ray Conference, Denver, 1, 330 (1973).

"Observations of the Time-Variations and Anisotropy of 0.16 to 3 MeV Electrons", G. J. Hurford, R. A. Mewaldt, E. C. Stone, and R. E. Vogt, Conf. Papers, 13th Int'l Cosmic Ray Conference, Denver, 1, 334 (1973).

"Observations of Low Energy Hydrogen and Helium Isotopes during Solar Quiet Times", G. J. Hurford, R. A. Mewaldt, E. C. Stone, and R. E. Vogt, Conf. Papers, 13th Int'l Cosmic Ray Conference, Denver, 1, 93 (1973).

"Measurements of the Flux of Low-Energy Solar-Flare Positrons", G. J. Hurford, R. A. Mewaldt, E. C. Stone, and R. E. Vogt, Conf. Papers, 13th Int'l Cosmic Ray Conference, Denver, 2, 1613 (1973).

"Observations of H and He Isotopes in Solar Cosmic Rays", G. J. Hurford, R. A. Mewaldt, E. C. Stone, and R. E. Vogt, Bull. Am. Astron. Soc., Part II, 6, 270 (1974).

"Observations of Low-Energy Hydrogen and Helium Nuclei during Solar Quiet Times", G. J. Hurford, R. A. Mewaldt, E. C. Stone, and R. E. Vogt, Bull. Am. Astron. Soc., Part II, 6, 274 (1974).

"The Time Variation of 5-11 MeV/nucleon Cosmic Ray Nitrogen and Oxygen Nuclei", R. A. Mewaldt, E. C. Stone, and R. E. Vogt, Bull. Am. Phys. Soc., 19, 433 (1974).

"The Isotopic Composition of 5 to 12 MeV/nucleon Cosmic Ray Nitrogen and Oxygen Nuclei", G. J. Hurford, R. A. Mewaldt, E. C. Stone, S. B. Vidor, and R. E. Vogt, Bull. Am. Phys. Soc., 19, 433 (1974).

"The Energy Spectrum of 0.16 to 2 MeV Electrons during Solar Quiet Times", G. J. Hurford, R. A. Mewaldt, E. C. Stone, and R. E. Vogt, Ap. J., 192, 541 (1974).

"Observations of Low Energy Hydrogen and Helium Isotopes during Solar Quiet Times", G. J. Hurford, R. A. Mewaldt, E. C. Stone, and R. E. Vogt, presented at the 2nd Cosmic Ray Isotope Symposium, Durham, N. H., October 1974.

"Isotopic Composition of 6-12 MeV/nuc Cosmic Ray Nitrogen and Oxygen", R. A. Mewaldt, E. C. Stone, S. B. Vidor, and R. E. Vogt, presented at the 2nd Cosmic Ray Isotope Symposium, Durham, N. H., October 1974.

"Isotopic Calibration of a dE/dx-E Telescope", R. A. Mewaldt, E. C. Stone, S. B. Vidor, and R. E. Vogt, presented at the 2nd Cosmic Ray Isotope Symposium, Durham, N. H., October 1974.

"Solar Cosmic Ray Observations of Hydrogen and Helium Isotopes", G. J. Hurford, E. C. Stone, and R. E. Vogt, presented at the 2nd Cosmic Ray Isotope Symposium, Durham, N. H., 1974.

"The Anomalous Low-Energy Cosmic Rays: Local or Interstellar?", R. A. Mewaldt, Invited Paper, Anaheim APS Meeting, Bull. Am. Phys. Soc., 20, 52 (1975).

"Observations of Hydrogen and Helium Isotopes in Low-Energy Cosmic Rays", R. A. Mewaldt, E. C. Stone, and R. E. Vogt, Bull. Am. Phys. Soc., 20, 709, (1975).

"The Elemental Composition of Cosmic Rays with 3-30 MeV/nuc", E. C. Stone, R. A. Mewaldt, S. B. Vidor, and R. E. Vogt, ibid, 20, 633 (1975).

"The Puzzle of ^{3}He Rich Solar Flares", E. C. Stone, Invited Paper, Washington APS Meeting, April 1975, Bull. Am. Phys. Soc., 20, 680 (1975).

"A Search for Solar Flare Positrons", R. A. Mewaldt, E. C. Stone, and R. E. Vogt, 14th Int'l Cosmic Ray Conference, Munich, Germany, Conf. Papers, Vol. 5, p. 1668, (1975).

"Implications of Time Variations for the Origin of Low Energy Cosmic Ray Nitrogen and Oxygen Nuclei", R. A. Mewaldt, E. C. Stone, and R. E. Vogt, 14th Int'l Cosmic Ray Conference, Munich, Germany, Conf. Papers, Vol. 2, p. 798, (1975).

"The Quiet Time Spectra of Low-Energy Hydrogen and Helium Nuclei", R. A. Mewaldt, E. C. Stone, and R. E. Vogt, 14th Int'l Cosmic Ray Conference, Munich, Germany, Conf. Papers, Vol. 2, p. 774, (1975).

"The Isotopic Composition of Hydrogen and Helium in Low-Energy Cosmic Rays", R. A. Mewaldt, E. C. Stone, and R. E. Vogt, 14th Int'l Cosmic Ray Conference, Munich, Germany, Conf. Papers, Vol. 1, p. 306, (1975).

"Observations of Low Energy Interplanetary Electrons", R. A. Mewaldt, E. C. Stone, and R. E. Vogt, 14th Int'l Cosmic Ray Conference, Munich, Germany, Conf. Papers, Vol. 2, p. 758, (1975).

"The Elemental Composition of 4 - 30 MeV/nuc Cosmic Ray Nuclei with $1 \leq Z \leq 8$", R. A. Mewaldt, E. C. Stone, S. B. Vidor, and R. E. Vogt, 14th Int'l Cosmic Ray Conference, Munich, Germany, Conf. Papers, Vol. 2, p. 798 (1975).

"Isotopic Composition of the Anomalous Low-Energy Cosmic Ray Nitrogen and Oxygen", R. A. Mewaldt, E. C. Stone, S. B. Vidor, and R. E. Vogt, 14th Int'l Cosmic Ray Conference, Munich, Germany, Conf. Papers, Vol. 1, p. 349 (1975).

"Observations of Hydrogen and Helium Isotopes in Solar Cosmic Rays", G. J. Hurford, E. C. Stone, and R. E. Vogt, 14th Int'l Cosmic Ray Conference, Munich, Germany, Conf. Papers, Vol. 5, p. 1624, (1975).

"The Quiet Time Flux of 0.16 - 1.6 MeV Cosmic Ray Positrons", R. A. Mewaldt, E. C. Stone, and R. E. Vogt, 14th Int'l Cosmic Ray Conference, Munich, Germany, Conf. Papers, Vol. 1, p. 401, (1975).

"Enrichment of Heavy Nuclei in ^{3}He Rich Flares", G. J. Hurford, R. A. Mewaldt, E. C. Stone, and R. E. Vogt, Astrophy. J., 201, L95-L97, (1975).

"The Isotopic Composition of Hydrogen and Helium in Low Energy Cosmic Rays", R. A. Mewaldt, E. C. Stone, and R. E. Vogt, Ap. J. 206, 616 (1976).

"Observations of Jovian Electrons at 1 AU", R. A. Mewaldt, E. C. Stone, and R. E. Vogt, JGR 81, 2397 (1976).

"Isotopic and Elemental Composition of the Anomalous Low Energy Cosmic Ray Fluxes", R. A. Mewaldt, E. C. Stone, S. B. Vidor, and R. E. Vogt, Ap. J.205, 931 (1976).

"Correlation of Electrons $E_e > 0.2$ MeV with Low Energy Electrons ($50 \text{ eV} \leq E_e \leq 50$ keV) in the Earth's Magnetotail", D. N. Baker, E. C. Stone, R. E. Vogt, K. L. Ackerson, and L. A. Frank, Trans. Am. Geo. Union, 56, 1046, (1975).

"Energetic Electrons Observed in Conjunction with Magnetotail Fireball Events", D. N. Baker, E. C. Stone, and R. E. Vogt, Trans. Am. Geo. Union, 57, 314 (1976).

"The Isotopic and Elemental Composition of ~4 to ~30 MeV/nucleon Cosmic Rays", R. E. Vogt, R. A. Mewaldt, and E. C. Stone, Bull. Am. Phys. Soc., 21, 540 (1976).

"Deuterium and ^{3}He in Low Energy Cosmic Rays", R. A. Mewaldt, E. C. Stone, and R. E. Vogt, ibid, 21, 641 (1976).

"Quiet Time Measurements of Low Energy Hydrogen and Helium Nuclei: 1972-1975", E. C. Stone, R.A. Mewaldt, and R. E. Vogt, ibid, 21, 641 (1976).

"Energetic Electron Anisotropies in the Magnetotail: Identification of Open and Closed Field Lines", D. N. Baker, E. C. Stone, Geophys. Res. Letters, 3, 557 (1976).

"High Energy Electrons (E ≥ 200 keV) Observed in the Magnetotail Boundary Layer", D. N. Baker and E. C. Stone, Trans. Am. Geo. Union, 57, 995 (1976).

"A Steady-State Model of Sunward Flow of Low Energy Protons", E. C. Stone and F. E. Marshall, Trans. Am. Geo. Union, 57, 980 (1976).

"Persistent Sunward Flow of ~ 1.6 MeV Protons at 1 AU", F. E. Marshall and E. C. Stone, Trans. Am. Geo. Union, 57, 980, (1976).

"Persistent Sunward Flow of ~ 1.6 MeV Protons at 1 AU", F. E. Marshall and E. C. Stone, Geophys. Res. Letters, 4, 57 (1977).

"Observations of Energetic Electrons (E ≥ 200 KeV) in the Earth's Magnetotail: Plasma Sheet and Fireball Observations", D. N. Baker and E. C. Stone, JGR 82, 1537 (1977).

"The Magnetopause Energetic Electron Layer Along the Distant Magnetotail", D. N. Baker and E. C. Stone, Geophys. Res. Letters, 4, 133 (1977).

"Observations of 1 to 6 MeV Electrons in 1976", S. R. Hartman, R. A. Mewaldt, E. C. Stone, and R. E. Vogt, Tucson Conference on Solar Terrestrial Physics, Jan. 1977.

"The Dependence of Sunward Streaming on the Interplanetary Magnetic Field", F. E. Marshall and E. C. Stone, ibid.

"Characteristics of α-Particles During Periods of Moderately Enhanced Proton Fluxes", E. C. Stone and F. E. Marshall, ibid.

"A Comparative Study of the Solar Modulation of the Anomalous Low Energy Cosmic Rays", R. A. Mewaldt, E. C. Stone, and R. E. Vogt, ibid.

"The Relationship of Energy Flow at the Magnetopause to Geomagnetic Activity" D. N. Baker and E. C. Stone, Geophys. Res. Letters 4, p.395, (1977).

"Radial Development of a Solar Cosmic Ray Event Between 0.4 and 1 AU on March 3, 1975 as Observed From Helios 1 and IMP-7", G. Wibberenz, H. Kunow, G. Green, R. Muller-Mellin, M. Witte, H. Hempe, R. A. Mewaldt, E. C. Stone, R. E. Vogt, and R. Reinhard, 15th Int'l. Cosmic Ray Conference, Plovdiv, Bulgaria, Conf. Papers, 5, 188 (1977).

"Persistent Sunward Flow of ~ 1.6 MeV Protons at 1 AU", F. E. Marshall and E. C. Stone, ibid 5, 197 (1977).

"Deuterium and ^{3}He in Low Energy Cosmic Rays", R. A. Mewaldt, E. C. Stone, R. E. Vogt, ibid 2, 321 (1977).

"Isotopic and Elemental Composition of Cosmic Rays Below ~ 30 MeV/nuc", R. A. Mewaldt, E. C. Stone, R. E. Vogt, ibid 2, 323 (1977).

"Temporal Variations in the Composition of Low Energy Cosmic Rays", R. A. Mewaldt, E. C. Stone, R. E. Vogt ibid 2, 322 (1977).

"Simultaneous Observations of Cosmic Ray Particles in Corotating Interplanetary Structures at Different Solar Distances Between 0.3 and 1.0 AU from HELIOS 1 and 2 and IMP 7 and 8", H. Kunow, G. Wibberenz, G. Green, R. Muller-Mellin, R. Witte, E. Hempe, E. C. Stone, R. A. Mewaldt and R. E. Vogt, ibid, Vol. 3 (1977).

"Neutral Particle Background in Cosmic Ray Telescopes Composed of Silicon Solid State Detectors", R. A. Mewaldt, E. C. Stone and R. E. Vogt, Space Science Instrumentation 3, 231-242 (1977).

"The Magnetopause Energetic Electron Layer 1, Observations Along the Distant Magnetotail", D. N. Baker and E. C. Stone, J. Geophys. Res. Vol 83, 4327 (1978).

"Characteristics of Sunward Flowing Proton and Alpha Particle Fluxes of Moderate Intensity", F. E. Marshall and E. C. Stone, J. Geophys. Res. Vol. 83, 3289 (1978).

"The Radial Diffusion Coefficient of 1.3 - 2.3 MeV Protons in Recurrent Proton Streams", R. A. Mewaldt, E. C. Stone and R. E. Vogt, Geophys. Res. Ltrs. 5, p. 965 (1978).

"Fast Electrons Near the Magnetopause and Their Dependence on Interplanetary Parameters", D. N. Baker, E. W. Hones and E. C. Stone, Trans. Am.Geo.Union 59, 365 (1978).

"The Streaming of Low Energy Protons Observed Between 1 and ~2.5 AU", A. C. Cummings, T. L. Garrard, E. C. Stone, R. E. Vogt and J. R. Jokipii, Bull. Am. Phys. Soc. 23, 508 (1978).

"The Radial Diffusion Coefficient of 1.3 - 2.3 MeV Protons During Recurrent Proton Streams", R. A. Mewaldt, E. C. Stone and R. E. Vogt, Bull. Am. Phys. Soc. 23, 509 (1978).

"Spectral Characteristics of Recurrent Proton and Alpha Particle Streams at 1 AU." R. A. Mewaldt, E. C. Stone, and R. E. Vogt, Bull. Amer. Phys. Soc. 23,509 (1978).

"Spectral and Temporal Characteristics of Solar Electrons from 20 keV to 20MeV." R. P. Lin, R. A. Mewaldt, E. C. Stone, R. E. Vogt, C. Paizis, M.A.I. van Hollebeke and R. E. Vogt, Bull. Amer. Phys. Soc. 23, 509 (1978).

"Characteristics of Recurrent Energetic Particle Events Observed Between 1 and ~4 AU", A. C. Cummings, T. L. Garrard, E. C. Stone, and R. E. Vogt, Trans. Am. Geo. Union 59,1153 (1978).

"Jovian Electron Increases at 1 AU and the Large Scale Structure of the Interplanetary Medium", S.R. Hartman, E.C. Stone, and R.E. Vogt, Trans. Am. Geo. Union 59, 1173 (1978).

"Characteristics of the Spectra of Protons and Alpha Particles in Recurrent Events at 1 AU", R. A. Mewaldt, E. C. Stone and R. E. Vogt, Geophys. Res. Ltrs., 6, 589 (1979).

"Energetic Electron Bursts in the Magnetopause Electron Layer and Interplanetary Space", J. W. Bieber and E. C. Stone, Trans. Am. Geo. Union 60, 369 (1979).

"Energetic Electron Bursts in the Magnetopause Electron Layer and in Interplanetary Space", J. W. Bieber and E. C. Stone, Proceedings of Magnetospheric Boundary Layers Conference, Alpbach, Austria, p. 131 (ESA SP-148, 1979).

"Simultaneous Two-Spacecraft Observations of the Magnetopause Electron Layer", J. W. Bieber and E. C. Stone, Trans. Am. Geo. Union 60, 909 (1979).

"Streaming Energetic Electrons in Earth's Magnetotail: Evidence for Substorm-Associated Magnetic Reconnection", J. W. Bieber and E. C. Stone, Geophys. Res. Ltrs. 7, 945 (1980).

"The Isotopic Composition of Cosmic Ray Carbon, Nitrogen, and Oxygen Nuclei", R. A. Mewaldt, J.D. Spalding, E. C. Stone and R. E. Vogt, Bull. Am. Phys. Soc. 25, 546 (1980).

"Open Field Lines in the Magnetotail and Their Relationship to Geomagnetic Activity", J. W. Bieber and E. C. Stone, EOS Trans. AGU 61, 344 (1980).

"Energetic Electrons Upstream of the Bow Shock and in the Magnetosheath", J. W. Bieber and E. C. Stone, Upstream Wave and Particle Workshop, JPL, April, 1980.

"Two-Spacecraft Observations of Energetic Electrons in Earth's Magnetotail", J. W. Bieber and E. C. Stone, ISEE Geomagnetic Tail Workshop, Seattle, March, 1981.

"A Two-Spacecraft Study of Substorm-Related Streaming Energetic Electrons", J. W. Bieber, and E. C. Stone, EOS Trans. AGU 62, 369 (1981).

"The Isotopic Composition of Low Energy Cosmic Rays", R. A. Mewaldt, J. D. Spalding, E. C. Stone, and R. E. Vogt, 17th Int'l. Cosmic Ray Conference, Paris, France, Conf. Papers 2, 68 (1981) and 11, 431 (1981).

"The Energy Spectrum of 20 keV - 20 MeV Electrons Accelerated in Large Solar Flares", R. P. Lin, R. A. Mewaldt, and M. A. I. Van Hollebeke, 17th Int'l. Cosmic Ray Conference, Paris, France, Conf. Papers 3, 64 (1981).

"A Study of Temporal and Radial Dependencies of the Anomalous Helium and Oxygen Nuclei", W. R. Webber, F. B. McDonald, T. T. von Rosenvinge, and R. A. Mewaldt, 17th Int'l. Cosmic Ray Conference, Paris, France, Conf. Papers 10, 92 (1981).

"Plasma Behavior During Energetic Electron Streaming Events: Further Evidence for the Substorm-Associated Magnetic Reconnection", J. W. Bieber, E. C. Stone, E. W. Hones, Jr., D. N. Baker, and S. J. Bame, EOS Trans. AGU 62, 986 (1981).

"Energetic Electrons in the Magnetosheath and Upstream of the Bow Shock", J. W. Bieber, and E. C. Stone, J. Geophys. Res. 87, 85 (1982).

"The Energy Spectrum of 20 keV - 20 MeV Electrons Accelerated in Large Solar Flares", R. P. Lin, R. A. Mewaldt, and M.A.I. Van Hollebeke, Ap.J. 253, 949 (1982).

"Observations of Substorm-Associated Magnetic Reconnection", J. W. Bieber, E. C. Stone, E. W. Hones, Jr., D. N. Baker, and S. J. Bame, presented at 1982 Yosemite Conference on Origins of Plasmas and Electric Fields in the Magnetosphere, January, 1982.

"Reconnection - Associated Energization of Plasma Sheet Electrons", J. W. Bieber, E. C. Stone, E. W. Hones, Jr., D. N. Baker, S. J. Bame, and R. P. Lepping, EOS Trans. AGU 63, 418 (1982).

"Plasma Behavior During Energetic Electron Streaming Events: Further Evidence for Substorm-Associated Magnetic Reconnection", J. W. Bieber, E. C. Stone, E. W. Hones, Jr., D. N. Baker, and S. J. Bame, Geophys. Res. Ltrs. 9, 664 (1982).

"Microstructure of Magnetic Reconnection in Earth's Magnetotail", J. W. Bieber, E. C. Stone, E. W. Hones, Jr., D. N. Baker, S. J. Bame, and R. P. Lepping, submitted to J. Geophys. Res. (1982).

Ph.D. THESES

"Observations of Hydrogen and Helium Isotopes in Solar Cosmic Rays", G. J. Hurford, Ph.D. Thesis, CIT (1974).

"Observations of Nitrogen and Oxygen Isotopes in Low Energy Cosmic Rays", S. B. Vidor, Ph.D. Thesis, CIT (1975).

"The Streaming of 1.3 - 2.3 MeV Cosmic-Ray Protons During Periods Between Prompt Solar Particle Events", F. E. Marshall, Ph.D. Thesis, CIT (1976).

"Observations of 1 - 6 MeV Jovian Electrons at 1 AU and a Study of Their Propagation", S. R. Hartman, Ph.D. Thesis, CIT (1979).

DR/DS 004188

HEX DUMP OF a11114

FILE 1 RECORD 1 520 BYTES

(0)	00000001	00000001	FFFFFFF8	0000004E	00000001	00000001	00770525	00000000	00000000	00000000
(40)	00000000	00000000	00000000	00000000	00000000	00000000	00000000	00000000	00000000	00000000
(80)	00000000	00000000	00000000	00000000	00000000	00000000	00000000	00000000	00000000	00000000
(120)	00000000	00000000	00000000	00000000	00000000	00000000	00000000	00000000	00000000	00000000
(160)	00000000	00000000	00000000	00000000	00000000	00000000	00000000	00000000	00000000	00000000
(200)	00000000	00000000	00000000	00000000	00000000	00000000	00000000	00000000	00000000	00000000
(240)	00000000	00000000	00000000	00000000	00000000	00000000	00000000	00000000	00000000	00000000
(280)	00000000	00000000	00000000	00000000	00000000	00000000	00000000	00000000	00000000	00000000
(320)	00000000	00000000	00000000	00000000	00000000	00000000	00000000	00000000	00000000	00000000
(360)	00000000	00000000	00000000	00000000	00000000	00000000	00000000	00000000	00000000	00000000
(400)	00000000	00000000	00000000	00000000	00000000	00000000	00000000	00000000	00000000	00000000
(440)	00000000	00000000	00000000	00000000	00000000	00000000	00000000	00000000	00000000	00000000
(480)	00000000	00000000	00000000	00000000	00000000	00000000	00000000	00000000	00000000	00000000

HEX DUMP OF a11114

FILE 148 RECORD 119 360 BYTES

(0)	25000000	77000000	08000000	5A000000	6D010000	17000000	EBE28900	00000000	00000000	00000000
(40)	07000000	06000000	03000000	01000000	01000000	00000000	02000000	00000000	86000000	00000000
(80)	00000000	250D0000	340A0000	00000000	00000000	00000000	00000000	52469A5D	2346A343	00000000
(120)	233D9C56	A93CD54F	A93BD54F	763A9245	C13BD70E	00000000	613BC6BF	00000000	06440000	00000000
(160)	763CC0F1	0A3C173E	433B2561	763A9245	C13BD70E	CF3B6FB0	1F3BF5A0	E23AED91	822035F7	00000000
(200)	DB3F1BFC	453EC245	823ED6FE	693D2930	F33BD7B6	A03B2D55	00000000	493E8928	84411B76	8F416CE3
(240)	9340B3FD	92415EB7	8F4162D5	7A41F545	9F41BA6C	8E41C633	9F411823	924102E5	B041E3A7	0D44A3A9
(280)	BF3DBD2A	003DDE01	CF3C1887	423C0A7E	8C3B5EB5	623BA5BE	113CC9CF	733C13FF	943E4857	943E6B16
(320)	133E8BA1	953E2489	933E7CA1	8C3E6BD4	993E563A	903E02B7	993EEF16	923EB92E	643E0A0B	D33F23E8

D-30920
10/28/73 - 12/31/73

DUMP OF TAPE X-401

INPUT TAPE X-401 ON MS3
DATA INPUT H9 NF 37 SR 31 1 SR 31 LAST SR 37 1 SR 37 LAST

FILE	INPUT RECS.	DATA RECORDS INPUT	MAX. SIZE	READ ERROR SUMMARY PERM	ZERO B	SHORT	UNDEF.	INPUT RETRIES #RECS.	TOTAL#
1	1	0	0	1	0	0	0	1	8

FILE 31 RECORD 1 LENGTH 520BYTES

(0)	0000001F	00000001	FFFFFFF9	00000049	0000012D	00000001	006FD935	00000000	00000000	00000000
(40)	00000000	00000000	00000000	00000000	00000000	00000000	00000000	00000000	00000000	00000000
(80)	00000000	00000000	00000000	00000000	00000000	00000000	00000000	00000000	00000000	00000000
(120)	00000000	00000000	00000000	00000000	00000000	00000000	00000000	00000000	00000000	00000000
(160)	00000000	00000000	00000000	00000000	00000000	00000000	00000000	00000000	00000000	00000000
(200)	00000000	00000000	00000000	00000000	00000000	00000000	00000000	00000000	00000000	00000000
(240)	00000000	00000000	00000000	00000000	00000000	00000000	00000000	00000000	00000000	00000000
(280)	00000000	00000000	00000000	00000000	00000000	00000000	00000000	00000000	00000000	00000000
(320)	00000000	00000000	00000000	00000000	00000000	00000000	00000000	00000000	00000000	00000000
(360)	00000000	00000000	00000000	00000000	00000000	00000000	00000000	00000000	00000000	00000000
(400)	00000000	00000000	00000000	00000000	00000000	00000000	00000000	00000000	00000000	00000000
(440)	00000000	00000000	00000000	00000000	00000000	00000000	00000000	00000000	00000000	00000000
(480)	00000000	00000000	00000000	00000000	00000000	00000000	00000000	00000000	00000000	00000000

FILE 31 RECORD 240 LENGTH 520BYTES

(0)	0000001F	000000F0	00000007	00000049	00000136	00000018	006FDCD0	00000000	00000000	00000000
(40)	00000097	00000025	00000026	00000011	00000002	00000000	00000000	00000000	00000022	00000000
(80)	000145C6	0000155A	00001BAD	00000646	000017D1	00000464	00000000	00001C5F	00003547	000D5E92
(120)	0001AEC5	000D83A7	000D4AB8	000DAAF1	000EAEC3	000D6191	000F06F9	000DADFB	000FDE8C	027E2A80
(160)	00000BAD	000002FD	0000026F	00000125	00000242	000000F5	000000C5	000001A1	000025A0	000023CE
(200)	00000CB3	000023FF	000023B3	00002646	000025C1	000023D2	000025F5	00002437	00001B95	00010885
(240)	00000000	00000CAB	00000852	00000000	00000000	00000000	00000000	43CAB999	43852FC8	00000000
(280)	40392DF6	3F876E1E	3F458B93	3F10F869	3EC85595	00000000	00000000	00000000	3EB447F7	00000000
(320)	3F4A6299	3F1643BB	3EB481F1	3E41DACD	3E8DA85F	3E6BC228	3E35E114	3E1D637F	3E13BC5D	00000000
(360)	40F71B50	401032D1	4014FEA4	3F4C2E57	40121080	3F3553A3	00000000	401585D3	41A04C3A	41A24159
(400)	41146BF8	41A40368	41A15068	41A5E03C	41B23179	41A265B7	41B66009	41A6051D	41C0984B	431E40F9
(440)	3F8DBF4E	3F244ABB	3F1D935F	3EDE89FD	3F1B6F4D	3EBA3084	3E959C53	3F13C87F	401C8A9D	401B28C1
(480)	3F9A2A16	401B4E52	401B148F	401D08A8	401CA31F	401B2BCC	401CCB3C	401B78F4	4014EC4C	40C8A4F4

FILE	INPUT RECS.	DATA RECORDS INPUT	MAX. SIZE	READ ERROR SUMMARY PERM	ZERO B	SHORT	UNDEF.	INPUT RETRIES #RECS.	TOTAL#
31	240	241	520	0	0	0	0	1	1

FILE 37 RECORD 1 LENGTH 520BYTES

(0)	00000025	00000001	00000007	00000049	00000169	00000001	006FF0A5	00000000	00000000	00000000
(40)	00000001	00000000	00000001	00000001	00000000	00000000	00000000	00000000	00000021	00000000
(80)	0000781C	00000F39	00001B95	00000A5A	0000006E	00000000	00000000	00001CA9	000D095A	000E1708
(120)	00016EB7	000DFFF2	000DBD5E	000EEB14	000F667E	000DFE0C	000FE09B	000E7B41	0010EFD9	027C9430
(160)	00000720	00000289	0000026D	0000017A	0000004E	00000064	000000C7	000001A5	00002672	00002531
(200)	00000BB8	000024DD	000024F0	00002830	0000266D	000024DB	00002705	00002543	00001C89	00010688
(240)	00000000	00000C8B	00000A6C	00000000	00000000	00000000	00000000	43C8B332	43A6C824	00000000
(280)	3E61D4CF	00000000	3E1D93E0	3E10221D	00000000	00000000	00000000	00000000	3E8BBB83	00000000
(320)	3E61D4CF	3E6CD880	3E1D93E0	3E10221D	3EBA2ACB	3E6CD880	3E366C40	3E1DAF68	3E11B1EF	00000000
(360)	405B1B96	3FB8C82E	4014EC10	3F7DACF6	3E53FC83	00000000	00000000	4015BD6A	419E3718	41AB0000
(400)	41116297	41A9E7D6	41A6BFDA	41B50D79	41BAE747	41A9D0D3	41C0B14B	41AFC05A	41CD8D2D	431E2DB6
(440)	3F568000	3F1ECC07	3F1D7933	3F11F423	3E3B6327	3E4C5E63	3E971C4A	3F13FB98	401D29A1	401C3651
(480)	3F8E3DD5	401BF69C	401C04DC	401E7C10	401D2630	401BF4B7	401D98DF	401C4423	4015A53A	40C72296

FILE 37 RECORD 120 LENGTH 520BYTES

(0)	00000025	00000078	00000007	00000049	0000016D	00000018	006FF24C	00000000	00000000	00000000
(40)	0000006B	00000012	00000002	00000001	00000006	00000000	00000000	00000000	00000024	00000000
(80)	0000EE49	00000FCF	00001C05	0000074E	00001126	00000072	00000000	00001CF8	00CD3450	000DC80D
(120)	00019DC7	000DCB95	000D7411	000E7E3B	000F58BC	000DDBAC	000F9B24	000E2642	00105FAB	0269C0D0
(160)	00000A45	00000295	00000284	00000145	000001FA	00000051	000000D5	000001B0	000026B1	00002535

0-80110
1-1-86 - 12-31-86
IMP-J
73-078A-06B

DUMP OF TAPE IMP8OUT

INPUT TAPE IMP8OUT ON TA0
DATA INPUT H9 NF=37 FL=1=1=1 SR=37=1=1 SR=37 LAST 1 186 1

2

FILE 1 RECORD 1 LENGTH 360BYTES

(0)	01000000	01000000	F8FFFFFF	56000000	01000000	01000000	253A8300	00000000	00000000	00000000
(40)	00000000	00000000	00000000	00000000	00000000	00000000	00000000	00000000	00000000	00000000
(80)	00000000	00000000	00000000	00000000	00000000	00000000	00000000	00000000	00000000	00000000
(120)	00000000	00000000	00000000	00000000	00000000	00000000	00000000	00000000	00000000	00000000
(160)	00000000	00000000	00000000	00000000	00000000	00000000	00000000	00000000	00000000	00000000
(200)	00000000	00000000	00000000	00000000	00000000	00000000	00000000	00000000	00000000	00000000
(240)	00000000	00000000	00000000	00000000	00000000	00000000	00000000	00000000	00000000	00000000
(280)	00000000	00000000	00000000	00000000	00000000	00000000	00000000	00000000	00000000	00000000
(320)	00000000	00000000	00000000	00000000	00000000	00000000	00000000	00000000	00000000	00000000

FILE 1 RECORD 240 LENGTH 360BYTES

(0)	01000000	F0000000	F8FFFFFF	56000000	0A000000	18000000	C03D8300	00000000	00000000	00000000
(40)	00000000	00000000	00000000	00000000	00000000	00000000	00000000	00000000	00000000	00000000
(80)	00000000	00000000	00000000	00000000	00000000	00000000	00000000	00000000	00000000	00000000
(120)	00000000	00000000	00000000	00000000	00000000	00000000	00000000	00000000	00000000	00000000
(160)	00000000	00000000	00000000	00000000	00000000	00000000	00000000	00000000	00000000	00000000
(200)	00000000	00000000	00000000	00000000	00000000	00000000	00000000	00000000	00000000	00000000
(240)	00000000	00000000	00000000	00000000	00000000	00000000	00000000	00000000	00000000	00000000
(280)	00000000	00000000	00000000	00000000	00000000	00000000	00000000	00000000	00000000	00000000
(320)	00000000	00000000	00000000	00000000	00000000	00000000	00000000	00000000	00000000	00000000

FILE	INPUT RECS.	DATA RECORDS INPUT	MAX. SIZE	READ ERROR SUMMARY PERM	ZERO B	SHORT	UNDEF.	INPUT RETRIES #RECS.	TOTAL#
1	240	241	360	0	0	0	0	0	0

FILE 37 RECORD 1 LENGTH 360BYTES

(0)	25000000	01000000	F8FFFFFF	56000000	69010000	01000000	C5C68300	00000000	00000000	00000000
(40)	00000000	00000000	00000000	00000000	00000000	00000000	00000000	00000000	00000000	00000000
(80)	00000000	00000000	00000000	00000000	00000000	00000000	00000000	00000000	00000000	00000000
(120)	00000000	00000000	00000000	00000000	00000000	00000000	00000000	00000000	00000000	00000000
(160)	00000000	00000000	00000000	00000000	00000000	00000000	00000000	00000000	00000000	00000000
(200)	00000000	00000000	00000000	00000000	00000000	00000000	00000000	00000000	00000000	00000000
(240)	00000000	00000000	00000000	00000000	00000000	00000000	00000000	00000000	00000000	00000000
(280)	00000000	00000000	00000000	00000000	00000000	00000000	00000000	00000000	00000000	00000000
(320)	00000000	00000000	00000000	00000000	00000000	00000000	00000000	00000000	00000000	00000000

FILE 37 RECORD 110 LENGTH 360BYTES 86 365 160 365

(0)	25000000	6E000000	08000000	56000000	6D010000	1E000000	62C88300	00000000	00000000	00000000
(40)	02000000	00000000	00000000	00000000	00000000	00000000	00000000	00000000	2A000000	00000000
(80)	00000000	D9080000	47070000	00000000	00000000	00000000	00000000	0D46009C	E84567E0	00000000
(120)	8A3C75A7	00000000	00000000	00000000	00000000	00000000	00000000	00000000	7E3C30AA	00000000
(160)	443C2816	1A3CC643	9A3BC643	283BEF49	833CE6EC	1A3CC643	9A3BC643	283BEF49	633B643E	00000000
(200)	063F2FCA	493EC52D	433E7E60	763D7415	6C3B85A6	00000000	00000000	AA3ECC05	0B42AAE7	1E4299C2
(240)	B7400D42	21427AA9	1F424DF8	19420A16	314228AF	1F42E6D9	304272CB	22423BB1	404222F4	A544F97B
(280)	833DD0BC	203D6AF1	C93CD0C8	613C6DD2	6C3B85A6	D83B0B7E	473C66A5	C13CE653	013FD677	0A3F2C8D
(320)	493EC142	003FD629	0C3F1FE1	003F92E1	043F1C54	F83E1FE3	0A3F858C	023F7CB7	CC3F85AC	3D40A180

FILE	INPUT RECS.	DATA RECORDS INPUT	MAX. SIZE	READ ERROR SUMMARY PERM	ZERO B	SHORT	UNDEF.	INPUT RETRIES #RECS.	TOTAL#
37	110	111	360	0	0	0	0	0	0

EOJ DUMP STOPPED AFTER FILE 37 # OF PERMANENT READ ERRORS 0

START TIME 01/18/90 13:34:16 STOP TIME 01/18/90 13:38:26

$$